Interactive comment on "Integrated water system simulation by considering hydrological and biogeochemical processes: model development, parameter sensitivity and autocalibration" by Y. Y. Zhang et al.

Anonymous Referee #3
Received and published: 20 August 2015

The hydrological cycle and surface water quality are closely related to vegetation, soil and biogeochemical elements, which are strongly influenced by human activities. It is essential to quantify interactions among these components for watershed management. This research developed a comprehensive model, which is in great need to provide a tool for better understanding of system function.

Response: Thanks very much for your comments and careful review. We revised the manuscript carefully by following the comments from all the reviewers. All the changes were highlighted in blue color and marked by track changes. Acknowledgement was added in the revision.

One of my concern is the optimisation of the model structure, as sub-models were developed separately for different proposes. For example the biogeochemical module and crop growth module are site-specific, which may need detailed soil input. It is quite difficult to obtain in current soil datasets.

Response: Thanks very much for your comments. Indeed, the ecological process modules are site-specific while the hydrological cycle module and water quality process module are at the basin scale. The solution of different spatial scales is one of important issues for the integration of different modules. In this study, we designed three levels of spatial calculation units, i.e., sub-basin, land-use and crop. The crop and land-use units were approximate to the site or field scale for the ecological process module, while the sub-basin unit was suitable for the hydrological cycle module and water quality process modules. The outputs of different levels of units were exchanged based on the area percentage of units (See P13 L11-31).

The detail input datasets of underlying surface are helpful to improve the model performance, especially for HCM, SBM, CGM, and SEM. We can still obtain the main inputs of soil characteristics from the current soil datasets although the spatial resolution was not high. The other data were used the default values.

It may be helpful to show how to conduct model calibration and validation. The model is very comprehensive, and there 182 parameters in the model. It may have difficulty in determination of parameter values in practice. I hope the authors can add one paragraph in the discussion and show how the model is used in practice, and your perspectives in the model's optimisation and application.

Response: Thanks very much for your comments. As usual, for complicated models, sensitivity analysis needs to be conducted first before calibration so that only limited number of parameters need to be calibrated while default values are adopted for the rest parameters (See P12 L9-13; P17 L5-7). The model calibration and validation were specified in the Section 2.1.5, Fig. and P11 L29- P13 L2. Moreover, the equifinality was discussed in section 4.2 (See P23 L4- P24 L2).

In supplement 2.1, the 'accumulated heat' is actually effective temperature, i.e., average temperature minus a base temperature. The 'heat unit index' is actually the thermal time, which may be more understandable. I cannot see HUI ranges from 0 to 1 from S7, as PHUj may not equal to the accumulated HU over growing seasons.

Response: Thanks very much for your careful review and comments. The terminologies were revised accordingly. PHU_j is the required cumulative thermal time for crop j from sowing to maturity, and HU_k is the actual cumulative thermal time in each simulation year. Therefore, when HU_k equals PHU_j (HUI = 1), Crop j will be maturity (See P S2 L6-L14).

Integrated water system model considering hydrological and biogeochemical processes: model development, with parameter sensitivity and autocalibration

Y.Y. Zhang[1,*], Q.X. Shao[2,*], A.Z. Ye[3], H.T. Xing[1,4], and J.Xia[1]

[1] Key Laboratory of Water Cycle and Related Land Surface Processes, Institute of Geographic Sciences and Natural Resources Research, Chinese Academy of Sciences, Beijing, 100101, China.

[2] CSIRO Digital Productivity Flagship, Leeuwin Centre, 65 Brockway Road, Floreat Park, WA 6014, Australia.

[3] College of Global Change and Earth System Science, Beijing Normal University, 100875, Beijing, China.

[4] CSIRO Agriculture Flagship, GPO BOX 1666, Canberra, ACT 2601, Australia

Correspondence to: Y.Y. Zhang (zhangyy003@igsnrr.ac.cn) and

Q.X. Shao (quanxi.shao@cisro.au)

Abstract

Integrated water system modeling is a reasonable approach for obtaining scientific understanding of severe water crises faced in the world and for promoting the implementation of integrated river basin management. The time variant gain model (TVGM), which is a classic hydrological model, is based on the complex Volterra nonlinear formulation. TVGM has obtained good performance on runoff simulation in numerous basins, but is disadvantageous in predicting other water-related components. In this study, TVGM was extended to an integrated water system model by coupling multiple water-related processes in hydrology, biogeochemistry, water quality and ecology, and by considering the interference of human activities. Parameter sensitivity and autocalibration modules were developed to improve simulation efficiency. The

Shaying River Catchment, which is the largest, highly regulated and heavily polluted tributary in the Huai River Basin of China, was selected as the case study area. The key water-related components were simulated, including runoff, water quality, nonpoint source (or diffuse source) pollutant load, and crop yield. Results showed that the extended model simulated most components reasonably well. In particular, the simulated daily runoff series at most regulated and less-regulated stations matched well with the observations. The average correlation coefficient and coefficient of efficiency between the simulated and observed runoffs were 0.85 and 0.70, respectively. Both the simulated low and high flow events were improved when the dam regulation was considered, except the low flow simulation at Zhoukou and Huaidian Stations. The daily ammonium-nitrogen (NH_4-N) concentration, which is used as a key index in the water quality evaluation in China, was well captured with the average correlation coefficient of 0.67. Furthermore, the nonpoint source NH_4-N load and the corn yields were simulated for each administrative region and the results were reasonable compared with the data from the official report and statistical yearbooks, respectively. This study is expected to provide a scientific basis for the implementation of such a modeling practice for integrated river basin management.

1. Introduction

Severe water crises are global issues that have emerged as a consequence of the rapid development of the social economy, and include flooding, water shortages, water pollution and ecological degradation. These issues hinder the equitable development of regions by compromising the sustainability of vital water resources and ecosystems (Gleick, 1997). It is impossible to address these water-related problems within a single scientific discipline (e.g., hydrology, hydraulics, water quality or aquatic ecology) because of the complicated interconnections among the physical, chemical and ecological components of an aquatic ecosystem (Kindler, 2000; Biswas, 2004; Paola *et al.*, 2006). The paradigm of integrated river basin management may be a sensible solution at basin scale by focusing on the coordinated management of water resources in terms of social-economy, water quality and ecosystems. Correspondingly, integrated water system modeling is a reasonable practice for the simultaneous simulation of water-related components (flow regimes, nutrient loss, sediment and water quality), and is also an effective tool for supporting water resource allocation, environmental flow management and river restoration.

Integrated water system modeling has gained popularity in the last decades due to the rapid development of water-related sciences, computer sciences, earth observation technologies and the availability of open data. Moreover, models naturally tend to grow in complexity (Beven, 2006). The hydrological cycle has been widely accepted as a critical linkage among physical, biogeochemical and ecological processes, and energy fluxes at the basin scale (Wigmosta *et al.*, 1994; Singh and Woolhiser, 2002; Burt and Pinay 2005). For example, the physiological and ecological processes of vegetation affect evapotranspiration, soil moisture distribution and infiltration, and nutrient absorption and movement. On the contrary, soil moisture and nutrient content directly affect crop growth. Overland flow is a carrier of the pollutants to water bodies. Therefore, the variation patterns of water-related components and their causes at the basin scale should be analyzed by coupling all of these processes to capture the interactions and feedback between individual cycles. Furthermore, multidisciplinary research provides an effective way to enable breakthroughs in water system modeling by integrating the mature theories of water-related disciplines (e.g., accumulated temperature law for phenological development, Darcy's law for groundwater flow, Saint-Venant equation for flow routing, balance equation for mass and momentum, Richards' equation for unsaturated zone, Horton theory for infiltration, Penman-Monteith equation for evapotranspiration), with support from abundant data sources (e.g., high-resolution spatial information data, chemical and isotopic data from field experiments) (Singh and Woolhiser, 2002; Kirchner, 2006).

Several models have been developed by using mature models of different disciplines since the 1980s (Di Toro *et al.*, 1983; Brown and Barnwell 1987; Johnsson *et al.*, 1987; Hamrick, 1992; Li *et al.*, 1992; Abrahamsen and Hansen, 2000; Tattari *et al.*, 2001). A general review and discussion can be found in Singh and Woolhiser (2002). Owing to the complexity of the integrated system and the scale conflicts between different models, most existing models focus only on one or two major water-related processes. According to the model orientation, existing models can be categorized into three major classes. (i) Hydrological models emphasize the rainfall-runoff relationship and link with some dominating water quality and biogeochemical processes. As a result, these models generally show satisfactory performance in simulating major hydrological processes. Examples of widely accepted models include TOPMODEL (Beven and Kirkby, 1979), SHE (Abbott *et al.*, 1986), HSPF (Bicknell *et al.*, 1993), VIC (Liang *et al.*, 1994), ANSWERS (Bouraoui and Dillaha, 1996), HBV-N (Arheimer and Brandt 1998, and 2000), and HYPE (Lindström *et al.*, 2010). (ii)Water quality models focus on the migration and transformation processes of pollutants in water bodies. The models can obtain the high spatial and temporal resolutions of water quality variables in river systems by adopting multi-dimensional dynamic equations. However, these models simulate the overland processes of water and pollutants with difficulty. Typical models include WASP (Di Toro *et al.*, 1983), QUAL2E (Brown and Barnwell 1987) and EFDC (Hamrick, 1992). (iii) Biogeochemistry models have advantages in the simulation of the physiological and ecological processes of vegetation, and the vertical movements of nutrients and water in soil layers at the field or experimental catchment scales. Nevertheless, these models lack accurate hydrological features (Deng *et al.*, 2011). Thus these models are hard to simulate the movements of water, nutrients and their losses along flow pathways in the basin. Examples of the biogeochemistry models include SOILN (Johnsson *et al.*, 1987), EPIC (Sharpley and Williams, 1990), DNDC (Li *et al.*, 1992), Daisy (Abrahamsen and Hansen, 2000), and ICECREAM (Tattari *et al.*, 2001). Therefore, most models usually achieve good performances only on the oriented processes, and only approximate results for other processes outside of the model's focus.

SWAT is a typical integrated water system model that can simulate most water-related processes over long period at large scales (Arnold *et al.*, 1998). The model structure and functions of SWAT are considered landmark in the field of water system modeling. However, not all water-related processes can be well captured in practice because of the inaccurate descriptions of certain processes, such as the daily simulations of extreme flow events (Borah and Bera, 2004), soil nitrogen and carbon (Gassman *et al.*, 2007), and applicability in regulated basins (Zhang *et al.*, 2012). Particularly, SWAT applies two alternative approaches to simulate surface runoff, namely, the empirical soil conservation service (SCS) curve number method and the conceptual Green-Ampt infiltration model. The SCS equation is usually prioritized, but the applicability of the curve number is questioned (Rallison and Miller 1981). The Green-Ampt infiltration model is usually limited to the simulation of flow events at micro-scales (King *et al.*, 1999). Furthermore, SWAT has difficulty in accurately capturing the complicated dynamic processes of soil nitrogen and carbon compared with other biochemistry models (Gassman *et al.*, 2007). Therefore, several modified versions of SWAT were developed, such as SWIM which is based on the hydrological components from SWAT and the nutrient cycle components from the MATSALU model (Krysanova *et al.*, 1998), and SWAT-N which extend SWAT by adopting DNDC (Polhert *et al.* 2006, 2007).

The time variant gain model (TVGM) proposed by Xia (1991) is a lumped hydrological model based on the hydrological data from many different scale basins all over the world. In TVGM, the rainfall-runoff relationship is considered nonlinear with surface runoff coefficient that varies over time and is significantly affected by antecedent soil moisture. TVGM has strong mathematical basis because this nonlinear relationship is transformed into a complex Volterra nonlinear formulation. Wang *et al.* (2002) extended TVGM to a distributed model (DTVGM) by taking advantages of better computing facilities and available data sources. DTVGM is currently widely used in many basins with different scales and different climate zones to investigate the effect of human activities and climate change on runoffs, and obtained good simulation performances (Xia *et al.*, 2005; Wang *et al.*, 2009). However, DTVGM is confined to hydrological cycle studies and cannot be applied to the integrated river basin management because other water-related processes are not included, such as the water quality processes, ecological processes, soil biogeochemical processes.

Motivated by the requirements for the integrated river basin management, integrated water system model should be further developed to produce reasonable simulation in both water quantity and quality processes in the real basins with possibility to simulate more water-related processes, such as soil biogeochemistry, crop growth. In this study, we extend the simulation functions of DTVGM as an integrated water system model and improves the modeling practice of water-related components. Our specific objectives are as follows: (1) to integrate the detailed interactions and linkages among hydrological, water quality, soil biogeochemical and ecological processes, as well as the prevalent regulations of water projects at the basin scale; (2) to couple robust parameter analysis approaches with the integrated water system model to improve model performances; (3) to examine the applicability of the extended model on key water-related components in complex basins, e.g., flow regimes, nonpoint source (or called diffuse source) pools of nutrients, water quality variables in water body and crop yield.

2. Methods and material

2.1 Model framework

The proposed model includes seven major modules, namely the hydrological cycle module (HCM), soil biochemical module (SBM), crop growth module (CGM), soil erosion module (SEM), overland water quality module (OQM), water quality module of water bodies (WQM) and dam regulation module (DRM). The parameter analysis tool (PAT) is also designed for model calibration. The exterior exchange components connecting different modules are given in Figure 1. The more detailed descriptions of each module and its interactions with other modules are given in sub-sections 2.1.1 to 2.1.5. The main equations of each process are deferred to the appendix and supplementary materials for readers who are interested in the mathematical details.

The extended model is based on the hypothesis that the cycles of water and nutrients (N, P and C) are inseparable and act as the critical linkages among all the modules. The model takes full advantages of the existing models, i.e., the powerful interconnection of the hydrological model with other processes at a large spatial scale, the elaborative description of the ecological model on nutrient vertical movement in soil layers, and the elaborative description of the water quality model on nutrient movements along river networks. First, several key components that are simulated by the hydrological module, such as evapotranspiration, soil moisture, and flow, serve as critical linkages in all the modules (Section 2.1.1). Second, the soil biochemical processes determine the nutrient loads absorbed in the crop growth process (CGM) and migrated into water bodies as the nonpoint pollutant source (OQM and WQM). The accurate descriptions of soil biochemical processes are helpful in improving the simulation of water quality processes in responding to agricultural management (Section 2.1.2). Third, the hydrological module provides a function to describe the spatial connections among spatial calculation units to simulate the overland and in-stream movements of water and nutrients at the basin scale (Sections 2.1.1 and 2.1.3).

2.1.1 Hydrological cycle module (HCM)

TVGM is adopted to calculate the surface runoff yields for different land-use areas, such as forests, grasslands, water bodies, urban areas, unused land, paddy land, and dryland agriculture. The potential evapotranspiration is calculated by using Hargreaves' method (Hargreaves and Samani, 1982) because only the widely available daily maximum and minimum temperature data are used. The actual plant transpiration is expressed as a function of potential evapotranspiration and leaf area index, whereas soil evaporation is expressed as a function of potential evapotranspiration and surface soil residues (Neitsch *et al.*, 2011). The interflow and baseflow have linear relationships with the soil moisture in the upper and lower layers, respectively (Wang *et al.*, 2009). The infiltration from the upper to the lower soil layers is calculated by using storage routing methodology (Neitsch *et al.*, 2011). The Muskingum method or kinetic wave equation is used for river flow routing.

Figure 2 shows that shallow soil water from the hydrological cycle module is one of the major factors that connect the crop growth module (to control crop growth) and the soil biochemical module (to control the vertical migration and reaction of nutrients in the soil profile). Plant transpiration is also linked to the soil biochemical module (to provide energy for vertical migration of nutrients in the soil profile). The surface runoff is linked to the soil erosion, while the overland flow is connected to the overland water quality modules (to drive migration of nutrients and sediment along flow pathways), and water quality module for runoff routing in water bodies (rivers and lakes). Moreover, the hydrological cycle module provides the inflows of individual dams or sluices for the dam regulation module.

2.1.2 Ecological process modules

The ecological process modules contain the soil biochemical module and the crop growth module. The crop growth and soil biochemical processes directly affect the soil moisture, evapotranspiration, the nutrient transformation and loss from soil layers. Therefore, the model incorporates the water cycle, nutrient cycle, crop growth, and their key linkages.

2.1.2.1 Soil biochemical module (SBM)

The soil biochemical module simulates the key processes of Carbon (C), Nitrogen (N) and Phosphorus (P) dynamics in the soil profile, including decomposition, mineralization, immobilization, nitrification, denitrification, plant uptake and leaching. Different forms of nutrients (N and P) outputted from the soil biochemical module are connected to the crop growth module as the nutrient constraints of crop growth, and to the overland water quality module as the main nonpoint sources of pollutant to water bodies (Figure 3a).

Soil C and N cycle. The daily step decomposition and denitrification sub-models in DNDC are adopted to simulate the biogeochemical processes of C and N in the soil profile at field scale according to the crop pattern in actual situations (Li *et al.*, 1992). The decomposition and other oxidation processes are the dominant microbial processes in the aerobic condition. The three conceptual organic C pools are: the decomposable residue, microbial biomass and stable (humus). The decomposition of each C pool is treated as the first-order decay process with the individual decomposition modified by soil temperature and moisture, clay content, and C: N ratio. The major simulated processes of decomposition under aerobic condition are mineralization, immobilization, ammonia (NH_3) volatilization and nitrification. Mineralization or immobilization of mineral N (NH_4^+ and NO_3^-) is determined by the flow rate of SOC pools. NH_3 volatilization is controlled by the simulated NH_4^+ concentration, clay content, pH, soil moisture and temperature. NH_4^+ is oxidized to NO_3^--N during nitrification and nitrous oxide (N_2O) is emitted into the air during nitrification. Denitrification occurs under anaerobic condition, which is controlled by soil moisture, temperature, pH, and dissolved soil organic carbon content. The detailed descriptions are given in Appendix B and Li *et al.*, 1992.

Soil P cycle. The major processes of soil P cycle are simulated based on the study of Horst *et al.* (2001). Six P pools are considered, namely, three organic pools (stable and active pools for plant uptake, fresh pool associated with plant residue) and three mineral pools (soluble mineral, stable and active pools) as the consequence of mineralization, decomposition and sorption (Horst *et al*, 2001). The P dynamics processes were considered in Horst *et al.* (2001) and Neitsch *et al.* (2011) through modeling the P release from fertilizer, manure, residue, microbial biomass, humic substances, and P sorption by plant uptake.

Soil profile is divided into three layers, namely, surface (0-10 cm), and user defined upper and lower layers, all of which are consistent with the soil layers of hydrological cycle module to exchange the values of linkages (e.g., soil water) among different modules smoothly.

2.1.2.2 Crop growth module (CGM)

The crop growth module is developed based on EPIC crop growth model (Hamrick, 1992), which uses the concepts of daily accumulated heat units on phenological crop development, Monteith's approach for potential biomass, harvest index for partitioning grain yield, and stress adjustments for water, temperature and nutrient (N and P) availability in the root zone of the soil layers. It simulates total dry matter, leaf area index, root depth and density distribution, harvest index, and nutrient uptake, etc (Williams *et al.*, 1989; Sharpley and Williams, 1990). The crop respiration and photosynthesis drive the vertical movements of water and nutrient. In the crop growth module, the output of leaf area index is the main factor connecting the hydrological cycle module (to control the transpiration) and the crop residue left in the fields is the main source of organic matters (C, N and P) connecting to the soil biochemical module for soil biochemical processes, to the overland water quality module, and to the soil erosion module as one of the five constraint factors (Figure 3b).

2.1.3 Water quality process modules

The water quality process modules focus on the migration and transformation of water quality variables (e.g., sediment, different forms of nutrients, chemical oxygen demand: COD) along the flow pathways in the land surface and river system. The main modules are the soil erosion module for the sediment yield, the overland water quality module for the nonpoint source pollutant loss and migration from the soil layers to water bodies, and the water quality module for the migration and transformation of pollutants in water bodies (point and nonpoint source loads).

2.1.3.1 Soil erosion module (SEM)

The soil erosion by precipitation is estimated using the improved USLE equation (Onstad and Foster 1975) based on runoff outputted from the hydrological cycle module and crop management factor outputted from the crop growth module. The soil erosion module simulates sediment load for the overland water quality module to provide the carrier for the migration of insoluble organic matter along overland transport paths and water bodies (Figure 4a).

2.1.3.2 Overland water quality module (OQM)

This module simulates the overland loss and migration load of nonpoint source pollutants (e.g., sediment, insoluble and soluble nutrients, COD) for the water quality module of water bodies (Figure 4b). The main sources include the nutrient loss from soil layers and urban areas, the farm manure from livestock in rural areas. The nutrient loss from soil layers, as the primary nonpoint source in most catchments, is determined by the overland flow and sediment yield (Williams *et al.*, 1989) and the other sources are estimated by using the export coefficient method (Johnes, 1996). The overland migration processes contain the soluble pollutant migration with overland flow and the insoluble pollutant migration with sediment. All of these processes occur along the overland transport paths.

2.1.3.3 Water quality module of water bodies (WQM)

Point and nonpoint pollution sources are considered in the extended model. Point sources are directly added to the surface water in the model according to their geographic positions. Common point sources are urban water treatment plants or industrial plants.

Two modules are designed for different types of water bodies, such as, the in-stream water quality module and the water quality module of water impounding (reservoir or lake). The enhanced stream water quality model (QUAL-2E) (Brown and Barnwell 1987), is a comprehensive and versatile stream model that simulates the longitudinal movement and transformation of water quality variables in the branch streams. The model is centered at dissolved oxygen (DO) and can simulate up to 15 water quality variables including water temperature, DO, sediment, different forms of nutrients (N and P), COD (Figure 4c). The model is solved at the sub-basin scale rather than at the fine grid scale to maintain spatial consistent with the hydrological cycle module. The water quality outputs provide the water quality boundary of dams or sluices for the dam regulation module. The water quality module of water impounding assumes that water body is at the steady state and focuses on the vertical interaction of water quality. The main processes include water quality degradation and settlement, sediment resuspension and decay.

2.1.4 Dam regulation module (DRM)

Dams and sluices highly disturb flow regimes and associated water quality processes in most river networks. Thus, the dam and sluice regulation should be considered in water system models. The dam regulation module provides the regulated boundaries (e.g., water storage and outflow) to the hydrological cycle module for flow routing and to the water quality module of water bodies for pollutant migration.

Given that different types of dams and sluices are likely to show completely different regulation behaviors, we try to reproduce the common functionalities for the flood control or water supply dams in this module. Three methods are proposed for calculating the water storage and outflow of dams or sluices, namely, the measured outflow, controlled outflow with target water storage, and the relationship between outflow and water storage volume. The first method requires users to provide the measured outflow series during the simulation period. The second method simplifies the regulation rule of dam or sluice for long-term analysis by assuming that water is stored according to the usable water level during non-flooding season and the flood control level during flooding season. The redundant water is discharged. This method requires the characteristic parameters of dams or sluices including water storage capacities of dead, usable, flood control and maximum flood levels and the corresponding water surface areas. The third method is based on relationships among water level, water surface area, storage volume and outflow according to the design data of dam, or long-term observed data (Zhang *et al.*, 2013) (Appendix C).

2.1.5 Parameter analysis tool (PAT)

Parameter sensitivity analysis and calibration are important steps in the applications of highly parameterized models and are treated seriously, particularly for integrated water system models (Mantovan and Todini, 2006; Mantovan *et al.* 2007; McDonnell *et al.*, 2007). In the model, 78 lumped and 104 distributed parameters involve the hydrological, ecological and water quality processes. The distributed parameters are divided into 46 overland parameters, 18 stream parameters and 40 parameters of water projects (only for the sub-basin with reservoir or sluice) according to their spatial distribution. These parameter values are determined by the properties of overland landscape and soil, stream patterns, and water projects, respectively. Different spatial calculation units share many common parameter values if their properties are the same. The sensitive parameters and their ranges are determined first to reduce the parameter dimensions by parameter sensitivity analysis or according to user experiences. Their values are then calibrated by auto-optimization methods or manual adjustment to achieve optimal model performances, whereas the insensitive parameters remain constant.

Owing to high parameterization, an optimum result is hard to achieve by subjective selection and judgment; therefore, PAT is designed for parameter sensitivity analysis, autocalibration and model performance evaluation. Moreover, PAT is a part of the extended model (Figure 5). The algorithms include the parameter sensitivity method (latin hypercube one factor at a time: LH-OAT) (van Griensven *et al.*, 2006), auto-optimization methods such as particle swarm optimization (PSO) (Kennedy, 2010), genetic algorithm (GA) (Goldberg 1989) and shuffled complex evolution (SCE-UA) (Duan *et al.*, 1994). The five indices are provided to evaluate model performance including bias (*bias*), relative error (*re*), root mean square error (*RMSE*), correlation coefficient (*r*), and coefficient of efficiency (*NS*). These methods and indices can be selected by users on the basis of their specific requirements.

The interconnections between PAT and other modules are the parameter groups that need to be analyzed in sensitivity analysis and optimization, and the objective functions described by the evaluation indices of model performance. PAT randomly samples the parameter values from the multi-dimensional parameter spaces to the extended model to obtain the values of the objective function. For parameter sensitivity analysis, the sensitivity index of individual parameters is evaluated by comparing the variation of the objective function value along with the changes of parameter values. For parameter autocalibration, the good parameter groups are kept or updated following the particular criteria provided by the auto-optimization methods until the convergence criteria or maximum iterations are achieved.

2.2 Model operation

2.2.1 Multi-scale solution

The spatial heterogeneities of basin attributes and the different time scales used in individual processes cause inconsistent spatial and temporal scales in model integration (Blöschl and Sivapalan, 1995; Sivapalan and Kalma, 1995; Singh and Woolhiser, 2002). For the spatial scale, three levels of spatial calculation units are designed in the model, namely, sub-basin, land-use and crop from largest to smallest. These units are minimum polygons with similar hydrological properties, land-use types and agriculture crop cultivation patterns. The sub-basins are defined on the basis of DEM, the positions of gauges and water projects (dams or sluices), and are used in the hydrological cycle module (e.g., flow routing in both land and in-stream), overland water quality module, water quality module of water bodies and dam regulation module. Seven specific land-use units of each sub-basin are partitioned by the land-use classification (i.e., forest, grassland, water, urban, unused land, paddy land and dryland agriculture). The related modules are the hydrological cycle module (e.g., water yield, infiltration, interception and evapotranspiration) and soil erosion module. Moreover, several specific land-use units (paddy land and dryland agriculture, forest, grassland), where agricultural activities usually occur, are divided further into the crop units for detailed analysis of the impact of agricultural management on water and nutrient cycles. In the current version of the model, these four land-use units are divided into 10 specific categories of crop units: fallow for all these land-use units; grass for grassland unit; fruit tree and non-economic tree for forest unit; early rice and late rice for paddy unit; spring wheat, winter wheat, corn, and mixed dry crop for dryland agriculture unit. The crop unit category of a specific land-use pattern varies depending on crop cultivation structure and timing. The related modules are the soil biochemical module and the crop growth module. All of the outputs of the crop unit are summarized at the land-use unit scale, or sub-basin scale on the basis of the area percentage of different units.

For the temporal scale, it is practical to use a daily time-step as this is consistent with the underlying rainfall-runoff module and the data availability. The sub-daily time scale may improve the performance in some modules (e.g., SEM, WQM). However, most observations (e.g., climate data sets, soil nutrient availability, and water quality concentrations), are at daily time scale, thus leading to potential uncertainty or inability to downscale the observations into a sub-daily time scale. Moreover, the sub-daily module will increase model complexity compared to regional simulations, as it is quite hard to obtain the information at the regional scale. Thus most processes need to be simplified to fit regional research. Linear or nonlinear aggregation functions are used to transform different time scales to daily scale (Vinogradov *et al.*, 2011), such as exponential relation for flow infiltration and overland flow routing processes, soil erosion processes (A5, A6 and S32 in the appendices), and accumulative relation for the crop growth process (S7 in the supplementary material).

2.2.2 Basic datasets and spatial delineation

The indispensable datasets of the proposed model are GIS data, daily meteorological data series, social and economic data series, and dam attribute data. Several monitoring data series are further needed for model calibration, such as runoff and water quality series in river sections, soil moisture and crop yield at the field scale. Table 1 shows all of the detailed datasets and their usages.

The hydrological toolset of Arc GIS platform is used to delineate all the spatial calculation units and river system on the basis of DEM, land-use data. The sub-basin attributes (e.g., sub-basin location, evaluation, area, land surface slope and slope length) and flow routing relationship between sub-basins are obtained during this procedure.

2.3 Study area and model testing

In this study, the extended model was applied to a highly regulated and heavily polluted river basin of China. The simulated components contained daily runoff and water quality concentrations at some river cross-sections, spatial patterns of nonpoint source pollutant load and crop yield at sub-basin scale.

2.3.1 Study area

The Shaying River Catchment (112°45′~113°15′E, 34°20′~34°34′N), which is the largest sub-basin of the Huai River Basin in China, is selected as the study area (Figure 6a). The drainage area is 36,651 km^2 with a mainstream of 620 km. The average annual population (2003-2008) (Figure 6b) is 32.42 million, with rural population of 23.70 million. The average annual stocks (Figure 6c) are 8.30 million (big animals) and 178.42 million (poultries). The average annual use of chemical fertilizer (Figure 6d) is 1.55 million ton (N: 38%-51%, P: 16%-25%, K: 7%-12% and others: 16%-35%). The basin is located in the typical warm temperate, and semi-humid continental climate zone. The annual average temperature and rainfall are 14-16°C and 769.5 mm, respectively. The Shaying River is the most seriously polluted tributary with a pollutant load contribution of over 40% in the whole Huai River and is usually known as the water environment barometer of the Huai River mainstream. To reduce flood or drought disasters, 24 reservoirs and 13 sluices, whose regulation capacities are over 50% of the total annual runoff, have been constructed and fragmented river into several impounding pools.

2.3.2 Model setup

All data sets for model setup and calibration were collected from the government bureaus, official books or scientific references. The detailed descriptions were presented in Tables S2 and S3 of the supplementary material. The Shaying River Catchment was divided into 46 sub-basins. According to the land-use classification standard of China (CNS,2007), the main land use types were dryland agriculture (84.04%), forest (7.66%), urban (3.27%), grassland (2.68%), water (1.43%), paddy (0.91%), and unused land (0.01%).The soil input parameters (the contents of sand, clay and organic matter) were calculated on the basis of the percentage of soil types in each sub-basin. The main crops were early rice and late rice in the paddy land, and winter wheat and corn in the dryland agriculture. Their main agricultural management schemes (fertilize, plant, harvest and kill) were summarized by field investigation in the studies of Wang *et al*., (2008) and Zhai *et al.* (2014) (Table S3). Crop rotation and its management schemes were considered in the model by setting the start time, the duration of management and the fertilizer amounts. Only two fertilizations (base and additional fertilization) were considered in the model during the complete growth cycle of a certain crop. The areas of sub-basin, land-use and crop units ranged from 46.48 km^2 to 3771.15 km^2, from 0.04 km^2 to 2762.5 km^2, and from 3.73 km^2 to 2762.5 km^2, respectively.

The daily data series at 65 precipitation stations and six temperature stations were interpolated to each sub-basin from 2003 to 2008 by using the inverse distance weighting method and the nearest-neighbor interpolation method, respectively. The social and economic data (e.g., population and livestock in the rural area, chemical fertilizer amount) were calculated for each sub-basin on basis of the area percentage.

Moreover, 5 reservoirs, 12 sluices and over 200 wastewater discharge outlets were considered in the model according to their geographical positions. The farm manure from rural living and livestock farming were considered in the model as nonpoint source owing to their scattered characteristics and the deficiency sewage treatment facilities in rural areas.

2.3.3 Model evaluation

NH_4-N concentration is one of the widely used indices in assessing water quality condition in China (CSEPA, 2002). Thus, both the observation series of daily runoff and NH_4-N concentration were used to calibrate the model parameters. There were five regulated stations (Luohe, Zhoukou, Huaidian, Fuyang and Yingshang) and one less-regulated station (Shenqiu) which is the downstream station situated far from water projects.

We selected LH-OAT for parameter sensitivity analysis and SCE-UA for parameter calibration in PAT. The initial parameter values were randomly preset from the value ranges determined by their physical characteristics. The evaluation indices are *bias*, *r* and *NS* as a demonstration of model performance of the extended model. However, *NS* is sensitive to extreme value, outlier and number of data points and is not commonly applied in environmental sciences (Ritter and Muñoz-Carpena, 2013). Thus *NS* was not used to evaluate the NH_4-N concentration simulation. Furthermore, given that the real observed yields of nonpoint pollutant loads and crops were hard to collect for the whole catchment (Chen *et al.*,2014), their simulations were only evaluated preliminarily by using *bias* according to the statistical results from official reports or statistical yearbooks (Wang, 2011; Henan Statistical Yearbook, 2003, 2004 and 2005).

The model calibration was conducted step-by-step as follows. Hydrological parameters were calibrated first against the observed runoff series at each station from upstream to downstream, and then water quality parameters against the observed NH_4-N concentration series. The calibration and validation periods were from 2003 to 2005 and from 2006 to 2008, respectively. To reduce the dimensions of the calibration problem, we restricted SCE-UA to calibrate only the sensitive parameters as defined by LH-OAT, whereas other parameters remained constants. Weighting method was usually used to comprehensively handle different objectives (Efstratiadis and Koutsoyiannis, 2010). In this study, these objective functions were simply aggregated to single objectives (f_{runoff} and $f_{NH4\text{-}N}$) as

$$\begin{cases} f_{runoff} = \min[(|bias| + 2 - r - NS)/3] \\ f_{NH_4-N} = \min[(|bias| + 1 - r)/2] \end{cases} \quad (1)$$

because the case study was only a demonstration of the model performance.

Moreover, the effect of dam regulation in the integrated water system models was considered because of the high regulation in most rivers. The dam and sluice regulation usually disturbs the intra-annual distribution of flow events, such as, flattening high flow and increasing low flow. The simulation performances of high and low flow were separately evaluated, and the effectiveness of the DRM was tested by comparing the simulation with and without considering the regulation. The high and low flow was determined by the cumulative distribution function (CDF). A threshold of 50% was used for easy presentation, i.e., the flow was treated as high flow (or low flow) if its percentile was greater than (or smaller than) the threshold.

3. Results

3.1 Parameter sensitivity analysis

Nine sensitive parameters were detected for runoff simulation (Table 2): soil related parameters W_{fc} (field capacity), W_{sat} (saturated moisture capacity), K_r (interflow yield coefficient) and K_{sat} (steady state infiltration rate); TVGM parameters g_1 (basic surface runoff coefficient) and g_2 (influence coefficient of soil moisture) for surface runoff calculation; ground water recharge parameters K_g (baseflow yield coefficient) and T_g (delay time for aquifer recharge); and adjusted factor K_{ET} of evapotranspiration. All of these parameters controlled the main hydrological processes, in which soil water and evapotranspiration processes were distinctly important and explain 54.3% and 23.2% of the runoff variation, respectively.

For NH_4-N concentration simulation, more than 90% of observed NH_4-N concentration variations were explained by 14 sensitive parameters categorized into hydrological (59.28% of variation), NH_4-N (20.65% of variation) and COD (12.34% of variation) related parameters. The main explanations were that hydrological processes provided the hydrological boundaries that affected the nonpoint source pollutant load into rivers, the degradation and settlement processes of NH_4-N in water bodies (van Griensven *et al.*, 2002). NH_4-N concentration was further influenced by the settling and biological oxidation processes. Moreover, it was a competitive relationship between COD and NH_4-N to consume DO of water bodies in a certain limited level (Brown and Barnwell, 1987).

3.2 Hydrological simulation

The simulations fitted the observations well at all the stations from the midstream to downstream (Figure 7 and Table 3). The *biases* were very close to 0.0 at all the regulated stations except Zhoukou with an underestimation (0.24 for calibration and 0.41 for validation) and Luohe with an overestimation (-0.52 for validation). The obvious biases were caused by the calibration for obtaining the optimal solution of the average of three evaluation indices, rather than the *bias* only. The *r* values ranged from 0.75 (Luohe for validation) to 0.92 (Yingshang for calibration) with an average value of 0.85, whereas the *NS* values ranged from 0.51 (Luohe for validation) to 0.84 (Yingshang for calibration) with an average value of 0.70. The results of the regulated stations were a little worse than those of the less-regulated station (Shenqiu) owing to the regulation.

By comparing the simulation results with the observations from 2003 to 2008, we can see that the high and low flows were usually overestimated at all stations if the model did not consider the regulations (Figure 8). Except the high flow events at Zhoukou, both high and low flow events at all the stations were simulated well when the dam and sluice regulation was considered (Table 4). The best fitting was at Fuyang, particularly for the high flow simulation (*bias*=0.10, *r*=0.89 and *NS*=0.78). From unregulation to regulation settings, the improvements measured by f_{runoff} ranged from

-0.08 (Zhoukou) to -0.29 (Huaidian) for high flow simulation, from -0.05 (Zhoukou) to -0.31 (Huaidian) for average flow simulation, and from -1.97 (Fuyang) to -3.91 (Yingshang) for low flow simulation except Zhoukou (1.28). The improvements in the performance of low flow simulations were the most obvious. However, their performance still need to be improved further, particularly the underestimation at Zhoukou and Huaidian. The possible reasons were that, on the one hand, the applied evaluation indices (*r* and *NS*) were known to emphasize high flow simulation rather than the low flow simulation (Pushpalatha *et al.*, 2012) and the objective of autocalibration was to obtain the optimal solution for the average of three evaluation indices rather than the *bias* only. The slight sacrifice of *bias* improves the overall simulation performance evaluated by these three indices. One the other hand, the dam regulation module still could not fully capture the low flow events.

Furthermore, the model performances of monthly flows were even better, particularly for *r* and *NS*. The values of *r* ranged from 0.87 (Luohe for both calibration and validation) to 0.95 (Fuyang for calibration) with the mean of 0.92, whereas the values of *NS* ranged from 0.67 (Luohe for validation) to 0.94 (Shenqiu for validation) with the mean of 0.80. Zhang *et al.* (2013) reproduced the long-term monthly flows by SWAT at the same stations. Compared with existing results, the extended model improved the flow simulations at the downstream stations although it became a little worse at the upstream stations (Luohe and Zhoukou for calibration). In particular, the water volume and agreements with the observations (i.e., *bias* and *NS*) were well captured.

3.3 Water quality simulation

The simulated concentrations matched well with the observations according to the evaluation standard recommend by Moriasi *et al.* (2007) (Figure 9 and Table 5). The *r* values of all stations were over 0.60 except Zhoukou (0.56 for validation), Yingshang (0.49 for validation) and Shenqiu (0.41 for validation) with an average value of 0.67. The *bias* of all stations were considered as “acceptable” with a range from -0.27 (Fuyang for validation) to 0.29 (Zhoukou for calibration). The best simulation was at Luohe. The obvious discrepancies between the simulations and observations often appeared in the period from January to May because of the poor simulation performance of low flows. Although the *bias* between calibration and validation changed markedly at Fuyang and Yingshang, the model performances were still acceptable. The probable explanation was that the *bias* for corresponding runoff simulations at these two stations also changed.

Compared with the results without the consideration of regulation, the simulation results were significantly improved when the regulation was considered except at Fuyang for calibration. The decrease in $f_{NH4\text{-}N}$ value ranged from 0.10 (Huaidian for calibration) to 0.49 (Zhoukou for validation) although it was increased slightly at Fuyang for calibration (0.02). The regulation of dams and sluices played an important role in the water quality simulation. In the upper stream of Shaying River, the flow was small and the pollutant concentration decreased obviously because of the degradation and settlement of large water storage. In the downstream of Shaying River, the NH_4-N concentration increased because of the pollutant accumulation and the decreasing flow of dams and sluices owing to the regulation (Zhang *et al*., 2010). Therefore, the simulated concentrations without regulation were usually overestimated or higher than the simulation with regulation at the upstream stations (Luohe and Zhoukou), however, these concentrations were underestimated at the downstream stations (Huaidian, Fuyang and Yingshang). The largest simulation difference between with and without the regulation consideration appeared at Zhoukou.

The spatial pattern of average annual nonpoint source NH_4-N loads was shown in Figure 10a. The modeled annual yield rates ranged from 0.048 t km^{-2} $year^{-1}$ to 11.00 t km^{-2} $year^{-1}$ with an average value of 0.73 t km^{-2} $year^{-1}$. The yield of each administrative region was summarized from the sub-basin scale according to the area percentage of sub-basins in each administrative region. Compared with the statistical load of each administrative region based on the soil erosion, land use and fertilizer amount in the official report (Wang, 2011), the *bias* of simulated nonpoint source load in the whole region was 21.31% when the two regions with great *bias* (i.e., Fuyang and Pingdingshan) were excluded as outliers. The high load yield regions were in the middle of Pingdingshan, Xuchang, Zhengzhou, Fuyang and Zhoukou regions. The spatial pattern was significantly correlated with the distribution of paddy area (r=0.506, p<0.001) and rice yield (r=0.799, p<0.001) (Figures 10 b and c). The fertilizer loss in the paddy areas might be the primary contributor to the nonpoint source NH_4-N load, possibly because the average nitrogen loss coefficient in China was just 30%-70% in the paddy areas, which was higher than that in dryland agriculture (20%-50%) (Zhu, 2000; Xing and Zhu, 2000).

The observed average annual point source NH_4-N loads into rivers were approximately 4.70×10^4 t $year^{-1}$ in the Shaying River Catchment. This result was summarized from the collected data for model input. The nonpoint source load contributed 38.57% of the overall NH_4-N load on average from 2003 to 2005; this value was slightly higher than the statistical results (29.37%) given in the official report (Wang, 2011). Moreover, the contributions of the nonpoint source load at the stations ranged from 31.72% (Huaidian) to 47.13% (Shenqiu). Compared with the nonpoint source load of each administrative region in 2000, the simulated annual loads tended to increase from 2003 to 2005 except in the Kaifeng region. The yields of the Fuyang and Pingdingshan regions increased most evidently. The primary pollution source in the Shaying River Catchment was still the point source; however, the nonpoint source was also an important concern. The spatial characteristic of the Shaying River Catchment was that the high nonpoint source contribution in the upstream, and low nonpoint source contribution in the middle and downstream because the point source load emission was usually concentrated in this region. Therefore, compared with the results of Zhang *et al.* (2013), the overall simulation performance of NH_4-N concentration was also improved significantly by considering the detailed processes of nutrient in the soil layers.

3.4 Crop yield simulation

The simulated corn yield and its spatial pattern were shown in Figure 11. The average annual yields were summarized at sub-basin scale and ranged from 0.08 to 326.95 t km^{-2} $year^{-1}$ with the average value of 76.84 t km^{-2} $year^{-1}$. The yield of each administrative region was further summarized and compared with the data from statistical yearbooks from 2003 to 2005 (Henan Statistical Yearbook, 2003, 2004 and 2005) to test the simulation performance (See the inset of Fig.11). The high-yield regions were Luohe, Fuyang and Zhoukou in the middle and down reaches, whose primary land use were dryland agriculture (93.12%, 95.87% and 93.18%, respectively). The yields of Luohe, Nanyang, Kaifeng regions were well simulated. The total yield was underestimated in the whole basin with a *bias* of 19.93%. The discrepancies might be caused by the boundary mismatch between the administrative region and sub-basin, obvious spatial heterogeneities of human agricultural activities, and the inaccurate cropping patterns in such huge regions. A high-resolution remote sensing image and field investigation might improve the model performance.

4. Discussion

4.1 Comparison with other models

The evident difference between the extended model and existing models is that the water-related processes are considered as an integrated water system rather than isolated systems for individual processes. Integrated water system models provide significant scientific basis to reasonably describe the complex water-related processes in real basins. The model is also expected to simulate the critical water-related components simultaneously, especially to improve the simulation performance of water quantity and quality. The proposed model will be more beneficial to integrated river basin management than the existing models.

The results of the extended model can compete with those of the existing studies in the Huai River Basin. Several typical models have also been applied to simulate runoff and water quality, e.g., SWAT for monthly runoff and water quality simulation at the regulated stations (Zhang *et al.*, 2012), SWAT and Xinganjiang models for daily runoff simulation at the unregulated upstream stations (Shi *et al.*, 2013), and DTVGM for daily runoff simulation (Ma *et al.*, 2014). Different models showed generally comparable performance of runoff or water quality simulations. For SWAT, the f_{runoff} values were from 0.11 to 0.20 with a mean of 0.16 at the daily scale for the unregulated stations (Shi *et al.*, 2013), and from 0.09 to 0.75 with a mean of 0.32 at the monthly scale for the regulated stations (Zhang *et al.*, 2012); and $f_{NH\text{-}N}$ values ranged from 0.18 to 0.86 with a mean of 0.47 (Zhang *et al.*, 2012). For Xinganjiang model, the f_{runoff} values were from 0.13 to 0.21 with a mean of 0.16 at the daily scale for the unregulated stations (Shi *et al.*, 2013). For DTVGM, the f_{runoff} values were 0.14 and 0.21 at the daily scale in the calibration and verification periods, respectively at Bengbu station. However, the extended model performed better than SWAT, especially for the regulated runoff and water quality simulations (see Tables 4-6). Moreover, both the Xinanjiang model and DTVGM can only simulate the flow series at unregulated or less-regulated stations because they did not consider the dam regulation in the model frameworks.

4.2 Equifinality

Untill now, the detailed water-related processes are still ambiguous and hard to be deduced from strong physical foundations (Beven and Freer, 2001; Beven, 2006). Empirical equations are still adopted to approximate the physical processes with numerous unknown parameters, especially in the large scale models. Furthermore, model extension requires additional numbers of parameters to be defined and calibrated without additional observations (Beven, 2006). A single output variable of models is usually associated with multiple processes and many parameters. For instance, SWAT contains over 200 parameters (Arnold *et al.*, 1998) and DNDC has nearly 100 parameters (Li *et al.*, 1992). Pohlert *et al.*, (2006) reported that six hydrological and 12 N-cycle sensitive parameters were detected in SWAT-N for the simulation of water flow and N leaching. In our extended model, nine and 14 sensitive parameters were detected for runoff and NH_4-N simulation, respectively, including the soil related parameters, surface runoff, and baseflow parameters, evapotranspiration parameters, and the degradation and settling parameters of water quality variables (Table 3). Therefore, most existing models are subject to equifinality, which was more serious if more water -related processes were considered, or more sub-basins were delineated for the distributed models.

The utilization of more information and multiple performance measures for single predicted component would be helpful for alleviating the equifinality (Her and Chaubey, 2015). In the extended model, the independent calibration and validation data sets were specified in Table 1 and most widely-used measures of model performances were also provided in the PAT. In the case study, we employed several observation sources (e.g., runoff and water quality observations at different stations, the nonpoint pollutant source load and crop yield data), and three measures to evaluate model performance for the individual components (e.g., *bias*, *r* and *NS*). Nonetheless, to make full use of the existing data in practice, parameter sensitivity analysis would be an effective way to reduce dimensionality in model calibration, and to focus only on critical processes and parameters that are sensitive to model outputs (van Griensven *et al.*, 2006). Model autocalibration would be efficient to obtain the optimal simulations from numerous samples in multi-dimensional parameter spaces.

4.3 Model limitations

The extended model still has several limitations:

(1). The mathematical descriptions of groundwater, crop growth processes and agriculture management practices were still inaccurate. The current model focuses on the detailed descriptions of hydrological and nutrient cycle in the soil layers and water bodies and dam regulations. Satisfactory performances on water quantity and quality simulation were obtained in our case study. However, the applications in the simulation of the groundwater, nonpoint source pollution load, crop yield in the agriculture regions could still be further improved. Moreover, the stratification of water impounding in the water quality module should be considered if the high resolution data of terrain elevation in the dams or lakes is available.

(2). High parameterization was an inevitable issue because of its all-inclusive framework. The integrated water system model considers most of water-related processes in the hydrological, ecology and water quality subsystems. All processes were controlled by unmeasurable parameters because of their empirical and/or scale dependent nature (Her and Chaubey, 2015). Although parameter sensitivity analysis and calibration were widely used approaches to resolve the high parameterization issue, the equifinality and parameter uncertainty were still inevitable because of the insufficient observations, and the complex interactions among different subsystems.

5. Conclusions

In this study, an integrated water system model was primarily developed on the basis of TVGM hydrological model to address the complex water issues emerging in the basins. The model performance was demonstrated in the Shaying River Catchment of China. The model would provide a reasonable tool for the effective water governance by capturing several indicative components of water-related subsystems simultaneously including the hydrological components (e.g., soil water and evaporation, plant transpiration, runoff and water storage in the dams and sluices), water quality components (e.g., nonpoint source load, water quality concentrations in water bodies), and ecological components (crop yield) which could be calibrated if observations are available. The case study showed that the simulated runoffs at most stations fitted the observations well in the highly regulated Shaying River Catchment. All the evaluation criteria were acceptable for both the daily and monthly simulations at most stations. This model captured the variation of discontinuous daily NH_4-N concentration and properly simulated the spatial patterns of nonpoint source pollutant load and corn yield.

Owing to the heterogeneity of spatial data in large basins and insufficient observations of individual subsystems, not all the results were acceptable and several processes were still not well calibrated (low flow events, nonpoint source pollutant load, and crop yield, etc.). The model could also be improved by further considering more accurate humanity activities in the agricultural management, calibration of multi-component and model uncertainty analysis because of the interactions and tradeoffs among different processes. The over-parameterization and the reasonable initial conditions of parameters would also be treated carefully in applications. Advanced mathematic analysis technologies would benefit the future model development, such as multi-objective optimization algorithm.

Appendix A: Hydrological cycle module

The basic water balance equation is

$$P_i + SW_i = SW_{i+1} + Rs_i + Ea_i + Rss_i + Rbs_i + In_i \tag{A1}$$

where P is precipitation (mm); SW is soil moisture (mm); Ea is actual evapotranspiration (mm) including soil evaporation (E_s, mm) and plant transpiration (E_p, mm); Rs, Rss and Rbs is surface runoff, interflow and baseflow (mm), respectively; In is the vegetation interception (mm) and i is the time step (day).

E_s and E_p are determined by potential evapotranspiration (E_0, mm), leaf area index (LAI, m^2/m^2) and surface soil residues (rsd, t/ha) (Ritchie, 1972) as.

$$\begin{cases} E_a = E_t + E_s \le E_0 \\ E_p = \begin{cases} LAI \cdot E_0/3 & 0 \le LAI \le 3.0 \\ E_0 & LAI > 3.0 \end{cases} \\ E_s = E_0 \cdot exp(-5.0\times10^{-5} \cdot rsd) \end{cases} \quad \text{(A2)}$$

where E_0 is calculated by Hargreaves method (Hargreaves and Samani, 1982).

The surface runoff (Rs, mm) yield equation (TVGM; Xia *et al.*, 2005) is given as

$$Rs = g_1 \left(SW_u / W_{sat}\right)^{g_2} \cdot (P - In) \quad \text{(A3)}$$

where SW_u and W_{sat} are surface soil moisture and saturation moisture (mm), respectively; g_1 and g_2 are coefficients of basic runoff and soil moisture, respectively.

The interflow (Rss, mm) and baseflow (Rbs, mm) have linear relationships with the soil moisture of the upper and lower layers, respectively (Wang *et al.*, 2009) as

$$\begin{cases} Rss = k_{ss} \cdot SW_u \\ Rbs = k_{bs} \cdot SW_l \end{cases} \quad \text{(A4)}$$

where k_{ss} and k_{bs} are the yield coefficients of interflow and baseflow, respectively; SW_l is soil moisture of the lower layer (mm).

The infiltration from the upper to lower soil layers is calculated using storage routing methodology (Neitsch *et al.*, 2011) as

$$\begin{cases} W_{\inf} = (SW_u - W_{fc}) \cdot [1 - \exp(-t/T_{\inf})] \\ T_{\inf} = (W_{sat} - W_{fc})/K_{sat} \end{cases} \quad \text{(A5)}$$

where W_{inf} is water infiltration amount on a given day (mm); W_{fc} is soil field capacity (mm); t and T_{inf} are time step and travel time for infiltration (hrs), respectively; and K_{sat} is saturated hydraulic conductivity (mm/hr).

The calculation of overland flow routing is adopted from Neitsch *et al.* (2011) as

$$\begin{cases} Q_{overl} = (Q'_{overl} + Q_{stor,i-1}) \cdot \left[1 - \exp(-T_{retain}/T_{route})\right] \\ T_{route} = T_{overl} + T_{rch} = \dfrac{L_{overl}{}^{0.6} \cdot n_{overl}{}^{0.6}}{18 \cdot slp_{overl}{}^{0.3}} + \dfrac{0.62 \cdot L_{rch} \cdot n_{rch}{}^{0.75}}{A^{0.125} \cdot slp_{rch}{}^{0.375}} \end{cases} \quad \text{(A6)}$$

where Q_{overl} is the overland flow discharged into main channel (mm); Q'_{overl} is the lateral flow amount generated in the sub-basin (mm), $Q_{stor,i-1}$ is the lateral flow in the previous day (mm); T_{retain} is the retain time of flow (days); T_{route}, T_{overl} and T_{rch} are the routing times of the total flow, overland flow and river flow, respectively (days); L_{overl} and L_{rch} are the lengths of sub-basin slope and river, respectively (km); slp_{overl} and slp_{rch} are the slopes of sub-basin and river, respectively (m/m); n_{overl} and n_{rch} are the Manning's roughness coefficients for sub-basin and river, respectively (m/m); A is the sub-basin area (km^2).

Appendix B: Soil biochemical module

B.1 Soil temperature (Williams *et al.*, 1984):

$$T(Z,t) = \overline{T} + (AM/2 \cdot \cos[2\pi \cdot (t-200)/365] + TG - T(0,t)) \cdot \exp(-Z/DD) \quad \text{(B1)}$$

where Z is soil depth (mm); t is time step (days); $\overline{T}$ and TG are average annual temperature and surface temperature (°C), respectively; AM is the annual variation amplitude of daily temperature; DD is the damping depth of soil temperature (mm) given as

$$\begin{cases} DD = DP \cdot \exp\left\{(\ln(500/DP) \cdot [(1-\xi)/(1+\xi)]^2\right\} \\ DP = 1000 + 2500BD/[BD + 686\exp(-5.63BD)] \\ \xi = SW/[(0.356 - 0.144BD) \cdot Z_M] \\ TG_{IDA} = (1-AB) \cdot (T_{mx} + T_{mn})/2 \cdot (1 - RA/800) + T_{mx} \cdot RA/800 + AB \cdot TG_{IDA-1} \end{cases} \quad \text{(B2)}$$

where DP is maximum damping depth of soil temperature (mm); BD is soil bulk density (t/m^3); ζ is scale parameter; IDA is day of the year; AB is surface albedo; RA is daily solar radiation (ly).

B.2 C and N cycle (Li *et al.*, 1992):

Decomposition: The decomposition of resistant and labile C is described by the first order kinetic equation, viz.

$$d\mathrm{C}/dt = \mu_{CLAY} \cdot \mu_{C:N} \cdot \mu_{t,n} \cdot [S \cdot k_1 + (1-S) \cdot k_2] \quad \text{(B3)}$$

where μ_{CLAY}, $\mu_{C:N}$ and $\mu_{t,n}$ are the reduction factors of clay content, C: N ratio and temperature for nitrification, respectively; S is labile fraction of organic C compounds; k_1 and k_2 is the specific decomposition rates of labile faction and resistant fraction, respectively (day^{-1}).

The NH_4 amount absorbed by clay and organic matters (FIX_{NH4}, kg/ha) is estimated as

$$FIX_{NH_4} = [0.41 - 0.47 \cdot \log(NH_4)] \cdot (CLAY / CLAY_{\max}) \qquad \text{(B4)}$$

where NH_4 is NH_4^+ concentration in the soil liquid (g/kg). $CLAY$ and $CLAY_{\max}$ are clay content and the maximum clay content, respectively.

$$\begin{cases} \log(K_{NH_4}/K_{H_2O}) = \log(NH_{4m}/NH_{3m}) + pH \\ NH_{3m} = 10^{\{\log(NH_4) - (\log(K_{NH_4}) - \log(K_{H_2O})) + pH\} \cdot (CLAY/CLAY_{\max})} \\ AM = 2 \cdot (NH_3) \cdot (D \cdot t / 3.14)^{0.5} \end{cases} \qquad \text{(B5)}$$

where K_{NH4} and K_{H2O} are dissociation constants for NH_4^+:NH_3 equilibrium, H^+: OH^- equilibrium, respectively; NH_{4m} and NH_{3m} are NH_4^+ and NH_3 concentrations (mol/L) in the liquid phase, respectively; AM and D are accumulated NH_3 loss (mol/cm^2) and diffusion coefficients (cm^2/d^2), respectively.

The nitrification rate ($dNNO$, kg/ha/day) is a function of the available NH_4^+, soil temperature and moisture. N_2O emission is a function of soil temperature and soil NH_4^+ concentration, viz.:

$$\begin{cases} dNNO = NH_4 \cdot [1 - \exp(-K_{35} \cdot \mu_{t,n} \cdot dt)] \cdot \mu_{SW,n} \\ N_2O = (0.0014 \cdot NH_4 / 30.0) \cdot (0.54 + 0.51 \cdot T) / 15.8 \end{cases} \qquad \text{(B6)}$$

where K_{35} is the nitrification rate at 35 ºC (mg/kg/ha); $\mu_{sw,n}$ is soil moisture adjusted factor for nitrification.

Denitrification: The growth rate of denitrifier ($(dB/dt)g$, kg/ha/day) is proportional to their respective biomass, which is calculated with double Monod kinetics equation

$$\begin{cases} (dB/dt)_g = \mu_{DN} \cdot B(t) \\ \mu_{DN} = \mu_{t,dn} \cdot (u_{NO_3} \cdot \mu_{PH,NO_3} + u_{NO_2} \cdot \mu_{PH,NO_2} + u_{N_2O} \cdot \mu_{PH,N_2O}) \\ u_{N_xO_y} = u_{N_xO_y,\max} \cdot (C / K_{C,1/2} + C) \cdot (N_xO_y / K_{N_xO_y,1/2} + N_xO_y) \end{cases} \qquad \text{(B7)}$$

where B is the denitrifier biomass (kg); μ_{DN} is the relative growth rate of the denitrifiers; u_{NxOy} and $u_{NxOy,max}$ are the relative and maximum growth rates of NO_2^-, NO_3^- and N_2O denitrifiers. $K_{C,1/2}$ and $K_{NxOy,1/2}$ are the half velocity constants of C and N_xO_y, respectively. $\mu_{PH,NxOy}$ and $\mu_{t,dn}$ are the reduction factors of soil pH and temperature, respectively, and are given as

$$\begin{cases} \mu_{PH,NO_3} = 7.14 \cdot (pH - 3.8)/22.8 \\ \mu_{PH,NO_2} = 1.0 \\ \mu_{PH,N_2O} = 7.22 \cdot (pH - 4.4)/18.8 \\ \mu_{t,dn} = \begin{cases} 2^{(T-22.5)/10} & if\ T < 60°C \\ 0 & if\ T \geq 60°C \end{cases} \end{cases} \quad \text{(B8)}$$

The death rate of denitrifier ($(dB/dt)_d$, kg/ha/hr) is proportional to denitrifier biomass, viz.

$$(d\mathrm{B}/dt)_d = M_C \cdot Y_C \cdot B(t) \quad \text{(B9)}$$

where M_C and Y_C are maintenance coefficient of C (1/hr), maximum growth yield of soluble C (kg/ha/hr), respectively.

The consumption rates of soluble C and CO_2 production are calculated as

$$\begin{cases} d\mathrm{C}_{\mathrm{con}}/dt = (\mu_{DN}/Y_C + M_C) \cdot B(t) \cdot \mu_{SW,d} \\ d\mathrm{CO}_2/dt = dC_{con,t}/dt - (d\mathrm{B}/dt)_d \end{cases} \quad \text{(B10)}$$

where $\mu_{sw,d}$ is soil moisture adjusted factor for denitrification.

The NO_3^-, NO_2^-, NO and N_2O consumption are calculated as

$$d\mathrm{N}_x O_y/dt = (u_{N_xO_y}/Y_{N_xO_y} + M_{N_xO_y} \cdot N_x O_y / N) \cdot B(t) \cdot \mu_{PHN_xO_y} \cdot \mu_{t,dn} \quad \text{(B11)}$$

where M_{NxOy} and Y_{NxOy} are maintenance coefficient (1/hr), maximum growth yield on NO_3-, NO_2-,NO or N_2O (kg/ha/hr), respectively.

N assimilation is calculated on the basis of the growth rates of denitrifiers and the C: N ratio ($CNR_{D:N}$) in the bacteria, viz.

$$(dN/dt)_{ass} = (dB/dt)_g \cdot (1/CNR_{D:N}) \quad \text{(B12)}$$

The emission rates are the functions of adsorption coefficients of the gases in soils and to the air filled porosity of the soil, given as.

$$\begin{cases} P(N_2) = 0.017 + ((0.025 - 0.0013 \cdot AD) \cdot PA \\ P(N_2O) = [30.0 \cdot (0.0006 + 0.0013 \cdot AD) + (0.013 - 0.005 \cdot AD)] \cdot PA \\ P(NO) = 0.5 \cdot [(0.0006 + 0.0013 \cdot AD) + (0.013 - 0.005 \cdot AD) \cdot PA] \end{cases} \quad \text{(B13)}$$

where $P(N_2)$, $P(NO)$ and $P(N_2O)$ are the emission rates of N_2, NO, N_2O, respectively, during a day; PA and AD are the air-filled fraction of the total porosity and adsorption factor depending on clay content in the soil, respectively.

Nitrate leaching: The NO_3^- leaching rate is a function of clay content, organic C content and water infiltration in the soil layer as

$$Leach_{NO_3} = W_{\inf} \cdot \mu_{CLAY} \cdot \mu_{soc} \tag{B14}$$

where $Leach_{NO3}$ is the NO_3^- leaching rate; μ_{CLAY} and μ_{soc} are the influence coefficients of clay content and soil organic C, respectively.

B.3 P cycle

The descriptions of P mineralization, decomposition and sorption are adopted from Neitsch *et al.* (2011) and provided as the supplementary material.

Appendix C: Dam regulation module (Zhang *et al.*, 2013)

The water balance model is used to consider the inflow, outflow, precipitation, evapotranspiration, seepage and water withdraw of dam or sluice. The equation is:

$$\Delta V = V_{flowin} - V_{flowout} + V_{pcp} - V_{evap} - V_{seep} - V_{withd} \tag{C1}$$

where ΔV, V_{flowin} and $V_{flowout}$ are the water storage variation, water volumes of entering and flowing out, respectively (m^3), and are calculated by HCM; V_{pcp}, V_{evap} and V_{seep} are the precipitation, evaporation and seepage volumes, respectively (m^3), which are the functions of surface water area and water storage. V_{withd} is the water withdraw volume by human, which is the model input.

According to the design data of dams and sluices in China, there is a particular relationship among water level, storage and outflow. The outflow is determined by the water level or water storage volume. Thus, the relationships are described by equations.

$$\begin{cases} V_{flowout} = f'(V, H) \\ SA = f''(V, H) \end{cases} \tag{C2}$$

where V and H are the water storage volume and water level during a day, respectively; *f'()* and *f''()* are the functions which could be determined by statistical analysis methods (e.g., correlation analysis, linear or non-linear regression analysis, polynomial regression analysis and least squares fitting).

Appendix D: Evaluation indices of model performance

Bias: $$bias = \sum_{i=1}^{N}(O_i - S_i) \Big/ \sum_{i=1}^{N} O_i \quad \text{(D1)}$$

Relative error: $$re = \sum_{i=1}^{N} \frac{O_i - S_i}{O_i} \times 100\% \quad \text{(D2)}$$

Root mean square error: $$RMSE = \sqrt{\sum_{i=1}^{N}(O_i - S_i)^2 \big/ N} \quad \text{(D3)}$$

Correlation coefficient: $$r = \sum_{i=1}^{N}(O_i - \overline{O}) \cdot (S_i - \overline{S}) \Big/ \sqrt{\sum_{i=1}^{N}(O_i - \overline{O})^2 \cdot \sum_{i=1}^{N}(S_i - \overline{S})^2} \quad \text{(D4)}$$

Coefficient of efficiency: $$NS = 1 - \sum_{i=1}^{N}(O_i - S_i)^2 \Big/ \sum_{i=1}^{N}(O_i - \overline{O})^2 \quad \text{(D5)}$$

where O_i and S_i are the i^{th} observed and simulated values, respectively; $\overline{O}$ and $\overline{S}$ are the average observed and simulated values, respectively. N is the length of series.

Acknowledgements

This study was supported by the Natural Science Foundation of China (No. 41271005), the China Youth Innovation Promotion Association CAS (No. 2014041), the Key Project for the Strategic Science Plan in IGSNRR, CAS (No. 2012ZD003), the Endeavour Research Fellowship, China Visiting Scholar Project from China Scholarship Council, and the CSIRO Computational and Simulation Sciences Research Platform. The authors would like to thank Dr. Yongqiang Zhang, Mr. James R Frankenberger for their participation in our internal review procedure, Dr.Markus Hrachowitz and Dr. Christian Stamm for improving the quality and presentation of

the manuscript, and the anonymous reviewers for their valuable comments and suggestions.

References

Abbott, M.B, Bathurst, J.C., Cunge, J.A., O'Connell, P.E. and Rasmussen, J.: An Introduction to the European System: Systeme Hydrologique Europeen (SHE). *J. Hydrol.* 87: 61-77, 1986.

Abrahamsen, P., and Hansen, S. Daisy: an open soil-crop-atmosphere system model. *Environ. Modell. Softw.*, 15(3): 313-330, 2000.

Arheimer, B. and Brandt, M.: Modelling nitrogen transport and retention in the catchments of southern Sweden. *Ambio* 27(6):471-480, 1998.

Arheimer, B. and Brandt, M.: Watershed modelling of non-point nitrogen pollution from arable land to the Swedish coast in 1985 and 1994. *Ecol. Engin.* 14:389-404, 2000.

Arnold, J. G., Srinivasan, R., Muttiah, R. S., and Williams, J. R.: Large-area hydrologic modeling and assessment: Part I. Model development. *J. Am. Water Resour. Assoc.* 34(1):73-89, 1998.

Beven, K.J. and Kirkby, M.J.: A physically based variable contributing area model of basin hydrology. *Hydrol. Sci. Bull.* , 24(1):43-69, 1979.

Beven, K.J. A manifesto for the equifinality thesis. *J. Hydrol.*, 320(1-2):18-36, 2006.

Bicknell, B. R., Imhoff, J. C., Kittle, J. L., Donigian, A. S., and Johanson, R. C.: Hydrologic Simulation Program –FORTRAN (HSPF): User's Manual for Release 10. Report No. EPA/600/R-93/174. Athens, Ga.: U.S. EPA Environmental Research Lab, 1993.

Biswas, A.K. Integrated water resources management: A reassessment-A water forum contribution. *Water Inter.* 29:248 - 256, 2004.

Blöschl, G., Sivapalan, M. Scale issues in hydrological modelling: a review. *Hydrol. Process.*, 9(3 - 4): 251-290, 1995.

Borah, D. K., and Bera, M.: Watershed-scale hydrologic and nonpoint-source pollution models: Review of application. *Trans. ASAE* 47(3): 789-803, 2004.

Bouraoui,F., and Dillaha,T.A.:ANSWERS-2000: Runoff and sediment transport model. *J. Environ. Eng.*, 122(6): 493-502, 1996.

Brown, L. C. and Barnwel, T. O.: The enhanced stream water quality models QUAL2E and QUAL2E-UNCAS: documentation and user manual. Env. Res. Laboratory. US EPA, 1987.

Burt, T.P. and Pinay, G.: Linking hydrology and biogeochemistry in complex landscapes. *Prog. Phys. Geog.*, 29(3): 297-316, 2005.

Chen, Y., Song, X., Zhang, Z., Shi, P., and Tao, F.: Simulating the impact of flooding events on non-point source pollution and the effects of filter strips in an intensive agricultural watershed in China, *Limnology*, 16, 91–101, 2015. doi: 10.1007/s10201-014-0443-2.

China's national standard (CNS): *Current land use condition classification* (GB/T21010-2007), General administration of quality supervision, inspection and quarantine of China and Standardization administration of China, Beijing, China, 2007.

China State Environmental Protection Administration (CSEPA), (2002). *Environmental quality standards for surface water* -GB 3838-2002. Beijing: China Environmental Science Press. (In Chinese).

Deng, J., Zhu, B., Zhou, Z. X., Zheng, X. H., Li, C. S., Wang, T., and Tang, J. L.: Modeling nitrogen loadings from agricultural soils in southwest China with modified DNDC. *J. Geophys. Res.: Biogeosci.* (2005–2012), 116(G2), 2011.

Di Toro, D.M., Fitzpatrick, J.J., and Thomann, R.V.: Water quality analysis simulation program (WASP) and model verification program (MVP)-Documentation. Hydroscience, Inc., Westwood, NY, for U.S. EPA, Duluth, MN, Contract No. 68-01-3872, 1983.

Duan, Q., Sorooshian, S., and Gupta, V. K.: Optimal use of the SCE-UA global optimization method for calibrating watershed models. *J.Hydrol.*, 158(3): 265-284, 1994.

Efstratiadis, A. and Koutsoyiannis, D.: One decade of multi-objective calibration approaches in hydrological modelling: a review. *Hydrol. Sci. J.*, 55:58-78, 2010.

Gassman, P.W., Reyes, M.R., Green,C.H., and Arnold, A.G.: The soil and water assessment tool: historical development, applications, and future research directions. *T. ASABE*, 50: 1211-1250, 2007.

Gleick, P.H. Water in crisis: paths to sustainable water use. *Ecol. Appl.*, 8(3): 571-579, 1998.

Goldberg, D. E.: Genetic algorithms in search, optimization, and machine learning, Reading Menlo Park: Addison-Wesley, Massachusetts, USA, 1989.

Hamrick, J. M.: A three-dimensional environmental fluid dynamics computer code: theoretical and computational aspects, Special Report, The College of William and Mary, Virginia Institute of Marine Science, Virginia, USA, 317, 1992.

Hargreaves, G. H., and Samani, Z. A.: Estimating potential evapotranspiration. *J. Irrigat. Drain. Div.*, 108(3), 225-230, 1982.

Henan Statistical Yearbook in 2003, 2004 and 2005. China Statistics Press, Beijing.

Her, Y., and Chaubey, I.. Impact of the numbers of observations and calibration parameters on equifinality, model performance, and output and parameter uncertainty. *Hydrol. Process.*, 29:4220-4237, 2015.

Horst, W.J., Kamh, M., Jibrin, J.M. and Chude, V.O.: Agronomic measures for increasing P availability to crops, *Plant. Soil.* 237: 211-223, 2001.

Johnes, P.J.: Evaluation and management of the impact of land use change on the nitrogen and phosphorus load delivered to surface waters: the export coefficient modelling approach. *J. Hydrol.*, 183(3): 323-349, 1996.

Johnsson, H., Bergstrom, L., Jansson, P. E., and Paustian, K.: Simulated nitrogen dynamics and losses in a layered agricultural soil. *Agr. Ecosyst. Environ.*, 18(4), 333-356,1987

Kirchner J.W.: Getting the right answers for the right reasons: Linking measurements, analyses, and models to advance the science of hydrology. *Water Resour. Res*, 42(3), 2006. W03S04 doi: 10.1029/2005WR004362.

Kindler, J.: Integrated water resources management: the meanders. *Water Int.,* 25:312-319, 2000.

King, K. W., Arnold, J. G., Bingner, R. L. Comparison of Green-Ampt and curve number methods on Goodwin Creek watershed using SWAT. *Trans. ASAE*, 42(4), 919-925, 1999.

Kennedy, J.: Particle swarm optimization, Encyclopedia of Machine Learning. Springer USA, 760–766, 2010.

Krysanova, V., Mueller-Wohlfeil, D.I., Becker, A.: Development and test of a spatially distributed hydrological / water quality model for mesoscale watersheds. *Ecol. Model.*, 106, 261-289,1998.

Li, C., Frolking, S., Frolking, T.A.: A model of nitrous oxide evolution from soil driven by rainfall events: 1. Model structure and sensitivity. *J. Geophys. Res.* (1984–2012), 97(D9): 9759-9776, 1992.

Liang, X., D. P. Lettenmaier, E. F. Wood, and S. J. Burges: A Simple hydrologically based model of land surface water and energy fluxes for GSMs, *J. Geophys. Res.*, 99(D7), 14,415-14,428, 1994.

Lindström, G., Pers, C.P., Rosberg, R., Strömqvist, J., Arheimer, B.:. Development and test of the HYPE (Hydrological Predictions for the Environment) model - A water quality model for different spatial scales. *Hydrol. Res.* 41.3-4:295-319,2010.

Ma, F., Ye, A., Gong, W., Mao, Y., Miao, C., and Di, Z. An estimate of human and natural contributions to flood changes of the Huai River. *Global Planetary Change*, 119, 39-50, 2014.

Mantovan, P., and Todini, E.: Hydrological forecasting uncertainty assessment: Incoherence of the GLUE methodology, *J. Hydrol.*, 330, 368–381, 2006.

Mantovan, P., Todini, E. and Martina, M. L.V.: Reply to comment by Keith Beven, Paul Smith, and Jim Freer on "Hydrological forecasting uncertainty assessment: Incoherence of the GLUE methodology", *J. Hydrol.*, 338, 319–324, 2007.

McDonnell, J. J., Sivapalan, M., Vache, K., Dunn, S., Grant, G., Haggerty, R., Hinz, C., Hooper, R., Kirchner, J., Roderick, M.L., Selker, J., and Weiler, M.: Moving beyond heterogeneity and process complexity: A new vision for watershed hydrology, *Water Resour. Res.*, 43, W07301, doi:10.1029/2006WR005467,2007.

Moriasi, D. N., J. G. Arnold, M. W. Van Liew, R. L. Binger, R. D. Harmel, and T. Veith.: Model evaluation guidelines for systematic quantification of accuracy in watershed simulations, *T. ASABE*, 50(3), 885-900, 2007.

Neitsch, S., Arnold, J., Kiniry, J., Williams, J.R., 2011. *SWAT2009 Theoretical Documentation*. Texas Water Resources Institute, Temple, Texas.

Onstad, C. A. and Foster, G. R.: Erosion modeling on a watershed. *T.ASAE* 18(2):288-292, 1975.

Paola, C., Foufoula-Georgiou, E., Dietrich, W.E., Hondzo, M., Mohrig, D., Parker, G., Power, M.E., Rodriguez-Iturbe, I., Voller, V., Wilcock,P.: Toward a unified science of the Earth's surface: opportunities for synthesis among hydrology, geomorphology, geochemistry, and ecology. *Water Resour. Res*., 42, 2006. W03S10. DOI: 10.1029/2005WR004336.

Pushpalatha, R., Perrin, C., Le Moine, N., and Andréassian, V.: A review of efficiency criteria suitable for evaluating low-flow simulations. *J.Hydrol.*, 420-421, 171-182, 2012.

Rallison, R.E. and Miller.,N.: Past, present and future SCS runoff procedure. 353-364, 1981. In V.P. Singh (ed.). Rainfall runoff relationship. Water Resources Publication, Littleton, CO.

Ritchie, J.T.: A model for predicting evaporation from a row crop with incomplete cover. *Water Resour. Res*. 8:1205-1213, 1972.

Ritter.A, and Muñoz-Carpena, R.: Performance evaluation of hydrological models: Statistical significance for reducing subjectivity in goodness-of-fit assessments. *J. Hydrol.*, 480: 33-45, 2013.

Pohlert, T., L. Breuer, J.A. Huisman, and H.-G. Frede.: Integration of a detailed biogeochemical model into SWAT for improved nitrogen predictions-model development, sensitivity and uncertainty analysis. *Ecol. Model.* 203:215-228, 2006.

Pohlert, T., L. Breuer, J.A. Huisman, and H.-G. Frede. Assessing the model performance of an integrated hydrological and biogeochemical model for discharge and nitrate load predictions. *Hydrol. Earth Syst. Sci.* 11:997–1011, 2007.

Sharpley, A.N. and Williams, J.R.: EPIC-erosion/productivity impact calculator: 1. Model documentation. Technical Bulletin-United States Department of Agriculture, Agric. Res. Service, Washington DC, USA, 1990.

Shi, P., Chen, C., Srinivasan, R., Zhang, X., Cai, T., Fang, X., Qu, S., Chen, X., and. Li, Q.. Evaluating the SWAT model for hydrological modeling in the Xixian watershed and a comparison with the XAJ model. *Water Resour. Manag.*, 25(10), 2595-2612, 2011.

Singh,V.P. and Woolhiser, D.A.: Mathematical modeling of watershed hydrology. *J. Hydrol. Eng.*, 7(4): 270-292, 2002.

Sivapalan, M. and Kalma, J. D.: Scale problems in hydrology: contributions of the Robertson Workshop. *Hydrol. Process.*, 9(3-4), 243-250,1995.

Tattari, S., Bärlund, I., Rekolainen, S., Posch, M., Siimes, K., Tuhkanen, H. R., and Yli-Halla, M.: Modeling sediment yield and phosphorus transport in Finnish clayey soils. *Transactions of the ASAE*, 44(2), 297-307, 2001.

van Griensven, A., Meixner, T., Grunwald, S., Bishop, T., Diluzio, M., and Srinivasan, R.: A global sensitivity analysis tool for the parameters of multi-variable catchment models. *J.Hydrol.*, 324(1), 10-23,2006.

Vinogradov, Y. B., Semenova, O. M., and Vinogradova, T. A.: An approach to the scaling problem in hydrological modelling: the deterministic modelling hydrological system. *Hydrol. Process.*, 25(7), 1055-1073, 2011.

Wang, G. S., Xia J., Tan G., and Lu A.F.: A research on distributed time variant gain model: A case study on Chao River basin (in Chinese), *Prog. Geogr.,* 21(6), 573–582, 2002

Wang, G., Xia, J., and Chen, J.: Quantification of effects of climate variations and human activities on runoff by a monthly water balance model: A case study of the Chaobai River basin in northern China. *Water Resour. Res.*, 45, W00A11, doi:10.1029/2007WR006768,2009.

Wang, J.Q., Ma, W.Q., Jiang, R.F. and Zhang, F.S.: Analysis about amount and ratio of basal fertilizer and topdressing fertilizer on rice, wheat, maize in China. *Chin. J.Soil Sci..*, 39(2):329-333, 2008. (In Chinese)

Wang, X.: Summary of Huaihe River Basin and Shandong Peninsula Integrated Water Resources Plan, *China water resources*, 23,112-114,2011.

Wigmosta, M.S., Vail, L.W., and Lettenmaier,D.P.: A distributed hydrology-vegetation model for complex terrain. *Water Resour. Res.*, 30(6): 1665-1679, 1994.

Williams, J.R., Jones, C.A., and Dyke, P.T. Modeling approach to determining the relationship between erosion and soil productivity. *Trans. ASAE*, 27(1): 129-144, 1984.

Williams, J. R., Jones, C. A., Kiniry, J. R., and Spanel, D. A. The EPIC crop growth model. . *Trans. ASAE*, 32(2):497-511, 1989.

Xia, J., Wang, G.S., Tan, G., Ye, A.Z., and Huang, G. H.: Development of distributed time-variant gain model for nonlinear hydrological systems. *Sci. China: Earth Sci.,* 48(6), 713-723, 2005.

Xia, J.: Identification of a constrained nonlinear hydrological system described by Volterra Functional Series, *Water Resour. Res.*, 27(9): 2415−2420, 1991.

Xing, G. X., and Zhu, Z. L.: An assessment of N loss from agricultural fields to the environment in China. *Nutr. Cycl. Agroecosys.*, 57(1): 67-73, 2000.

Zhai, X.Y., Zhang, Y.Y., Wang X.L., Xia J. and Liang, T.: Non-point source pollution modeling using Soil and Water Assessment Tool and its parameter sensitivity analysis in Xin'anjiang Catchment, China. *Hydrol. Process*. 28, 1627-1640, 2014.

Zhang, Y.Y., Xia, J., Shao, Q.X., and Zhai, X.Y.: Water quantity and quality simulation by improved SWAT in highly regulated Huai River Basin of China. *Stoch. Env Res. Risk A.*, 27(1), 11-27, 2013.

Zhu, Z. L.: Loss of fertilizer N from plants-soil system and the strategies and techniques for its reduction. *Soil Environ. Sci.*, 9(1):1-6, 2000. (in Chinese)

Table 1. The data sets and their categories used in the model

Category	Data	Objectives	Controlled processes
GIS	DEM	Elevation, area, longitude and latitude, slopes and lengths of each sub-basin and channel	Hydrology and water quality
	Land use map	Land use types and their corresponding areas in each sub-basin	Hydrology, water quality and ecology
	Soil map	Soil physical properties of each sub-basin such as bulk density, texture, saturated conductivity	
Weather	Daily precipitation	Daily precipitation of each sub-basin	Hydrology
	Daily maximum and minimum temperature	Daily maximum and minimum temperature of each sub-basin	
Hydrology	Runoff or other hydrological component observations, etc.	Hydrological parameter calibration	Hydrology
Water quality	Urban wastewater discharge outlets and the discharge load	Model input of point source pollutant load	Water quality
	Water quality observations (concentration or load), etc.	Water quality parameter calibration	
Ecology	Crop yield, leaf area index, etc.	Ecological parameter calibration	Ecology
Economy	Basic economic statistical indictors	Populations, breeding stock of large animals and livestock, water withdrawal in each sub-basin	Hydrology and water quality
Water projects	Reservoir design data attribute parameters	Regulation rules of reservoirs or sluices	Hydrology
Agricultural management	Fertilization and irrigation types, timing and amount, time of seeding and harvest, and crop types	Agricultural management rules of each sub-basin	Water quality and ecology

Table 2 Sensitive parameters, their value ranges and relative importance for runoff and NH_4-N simulations

Variables	Range	Definition	Relative importance for runoff (%)	Relative importance for NH_4-N (%)
W_{fc}	0.20 to 0.45	Field capacity of soil	32.73	11.10
W_{sat}	0.45 to 0.75	Saturated moisture capacity of soil	11.68	11.83
g_1	0 to 3	Basic surface runoff coefficient	7.30	10.34
g_2	0 to 3	Influence coefficient of soil moisture	10.54	12.11
K_{ET}	0 to 3	Adjustment factor of evapotranspiration	23.21	10.71
K_{ss}	0 to 1	Interflow yield coefficient	9.55	3.20
T_g	1 to 100	Delay time for aquifer recharge	1.74	-
K_{bs}	0 to 1	Baseflow yield coefficient	2.91	-
K_{sat}	0 to 120	Steady state infiltration rate	0.33	-
R_d(COD)	0.02 to 3.4	COD deoxygenation rate at 20 °C	-	6.62
R_{set}(COD)	-0.36 to 0.36	COD settling rate at 20 °C	-	3.60
R_d(NH_4)	0.1 to 1	Bio-oxidation rate of NH_4-N at 20 °C	-	1.97
K_{set}(NH_4)	0 to 100	Settling rate of NH_4-N in the reservoirs	-	14.17
K_d(COD)	0.02 to 3.4	COD deoxygenation rate in the reservoirs at 20°C	-	2.12
K_d(NH_4)	0.1 to 1.0	Bio-oxidation rate of NH_4-N in the reservoirs at 20 °C	-	4.51
Total relative importance			100.00	92.27

Table 3 Runoff simulation results for regulated and less-regulated stations

Stations	Periods	Daily flow				Monthly flow			
		bias	r	NS	f	bias	r	NS	f
Regulated stations									
Luohe	Calibration	0.00	0.84	0.70	0.15	0.00	0.87	0.71	0.14
	Validation	-0.52	0.75	0.51	0.42	-0.52	0.87	0.67	0.33
Zhoukou	Calibration	0.24	0.87	0.73	0.21	0.24)	0.90	0.76	0.19
	Validation	0.41	0.79	0.55	0.36	0.41	0.91	0.70	0.26
Huaidian	Calibration	0.03	0.88	0.77	0.13	0.03	0.91	0.81	0.10
	Validation	0.12	0.76	0.54	0.27	0.12	0.87	0.70	0.18
Fuyang	Calibration	0.00	0.90	0.81	0.10	0.00	0.95	0.89	0.05
	Validation	0.14	0.88	0.76	0.17	0.14	0.94	0.86	0.11
Yingshang	Calibration	-0.13	0.92	0.84	0.12	-0.13	0.92	0.84	0.12
	Validation	0.16	0.87	0.74	0.18	0.16	0.93	0.82	0.13
Less–regulated stations									
Shenqiu	Calibration	0.00	0.91	0.82	0.09	0.00	0.94	0.88	0.06
	Validation	-0.13	0.83	0.67	0.21	-0.13	0.98	0.94	0.08

Table 4. The runoff simulation results at regulated stations with and without the dam regulation considered. Range means the difference of objective function value between regulations considered and not considered. If the range value is less than 0.0, then the simulation with regulation is better than that without regulation. Otherwise, the simulation without regulation is better.

Stations	Regulated capacity (%)	Flow event	Regulation considered				Regulation not considered				Range
			bias	r	NS	f	bias	r	NS	f	
Luohe	0.26	High	-0.16	0.97	0.92	0.09	-0.62	0.97	0.80	0.29	-0.20
		Low	-0.02	0.98	0.69	0.12	-1.46	0.99	-5.53	2.67	-2.55
		Average	-0.15	0.97	0.93	0.08	-0.68	0.96	0.82	0.30	-0.22
Zhoukou	1.31	High	0.21	0.98	0.93	0.10	-0.38	0.98	0.87	0.18	-0.08
		Low	1.00	0.00	-2.57	1.86	-0.64	0.99	-0.08	0.58	1.28
		Average	0.30	0.99	0.93	0.13	-0.41	0.98	0.89	0.18	-0.05
Huaidian	1.37	High	0.02	0.98	0.95	0.03	-0.64	0.98	0.68	0.32	-0.29
		Low	0.36	0.97	0.43	0.32	-1.51	0.98	-5.88	2.80	-2.48
		Average	0.06	0.98	0.96	0.04	-0.74	0.98	0.72	0.35	-0.31
Fuyang	2.21	High	0.04	0.98	0.96	0.03	-0.39	0.99	0.86	0.18	-0.15
		Low	0.17	0.99	0.87	0.10	-1.43	0.99	-3.78	2.07	-1.97
		Average	0.05	0.99	0.97	0.03	-0.50	0.99	0.88	0.21	-0.18
Yingshang	1.76	High	0.03	0.98	0.95	0.03	-0.44	0.99	0.86	0.20	-0.17
		Low	0.18	0.99	0.82	0.12	-1.77	0.95	-9.26	4.03	-3.91
		Average	0.05	0.99	0.96	0.03	-0.60	0.98	0.86	0.25	-0.22

Table 5. The comparison of NH_4-N simulation results between with and without dam regulation considered.

Stations	Periods	Regulated			Unregulated			Range	Ratio of nonpoint source load (%)
		bias	r	f	bias	r	f		
Regulated stations									
Luohe	Calibration	-0.02	0.93	0.05	-0.67	0.60	0.54	-0.49	46.10
	Validation	-	-	-	-	-	-		
Zhoukou	Calibration	0.29	0.61	0.34	-0.56	0.38	0.59	-0.25	44.54
	Validation	0.27	0.56	0.36	-1.35	0.66	0.85	-0.49	
Huaidian	Calibration	0.22	0.73	0.25	0.49	0.80	0.35	-0.10	31.72
	Validation	0.02	0.67	0.18	0.22	0.51	0.36	-0.18	
Fuyang	Calibration	0.28	0.78	0.25	0.26	0.80	0.23	0.02	33.12
	Validation	-0.27	0.76	0.26	-0.38	0.56	0.41	-0.15	
Yingshang	Calibration	0.24	0.79	0.23	0.25	0.58	0.34	-0.11	33.26
	Validation	-0.24	0.49	0.38	-0.76	0.62	0.57	-0.19	
Less-regulated stations									
Shenqiu	Calibration	0.13	0.62	0.26	-	-	-	-	47.13
	Validation	0.16	0.41	0.37	-	-	-	-	

List of Figure Captions

Figure 1. The model structure and the interactions among the major modules (1: hydrological part; 2: water quality part; 3: ecological part; 4: dam regulation part; 5: PAT).

Figure 2. The flowchart of HCM and the interactions with other modules**.**

Figure 3. The flowchart of SBM (a) and CGM (b) in the ecological part and the interactions with other modules.

Figure 4. The flowchart of SEM (a), OQM (b) and WQM (c) in the water quality part and the interactions with other modules.

Figure 5. The flowchart of PAT and its interactions with other modules.

Figure 6. The location of study area (a) and the digital delineation of sub-basin, point source pollutant outlets, rural population (b), animal stock (c) and fertilization (d).

Figure 7. The daily runoff simulation at all stations.

Figure 8. The cumulative distributions of simulated and observed daily runoff at all stations

Figure 9. The simulated NH_4-N concentration variation at all stations.

Figure 10. The spatial pattern of nonpoint source NH_4-N load (a) and its relationship with paddy area (b) and rice yield (c) at the sub-basin and regional scale in the Shaying River Catchment.

Figure 11. The spatial pattern of corn yield at the sub-basin and regional scale in the Shaying River Catchment.

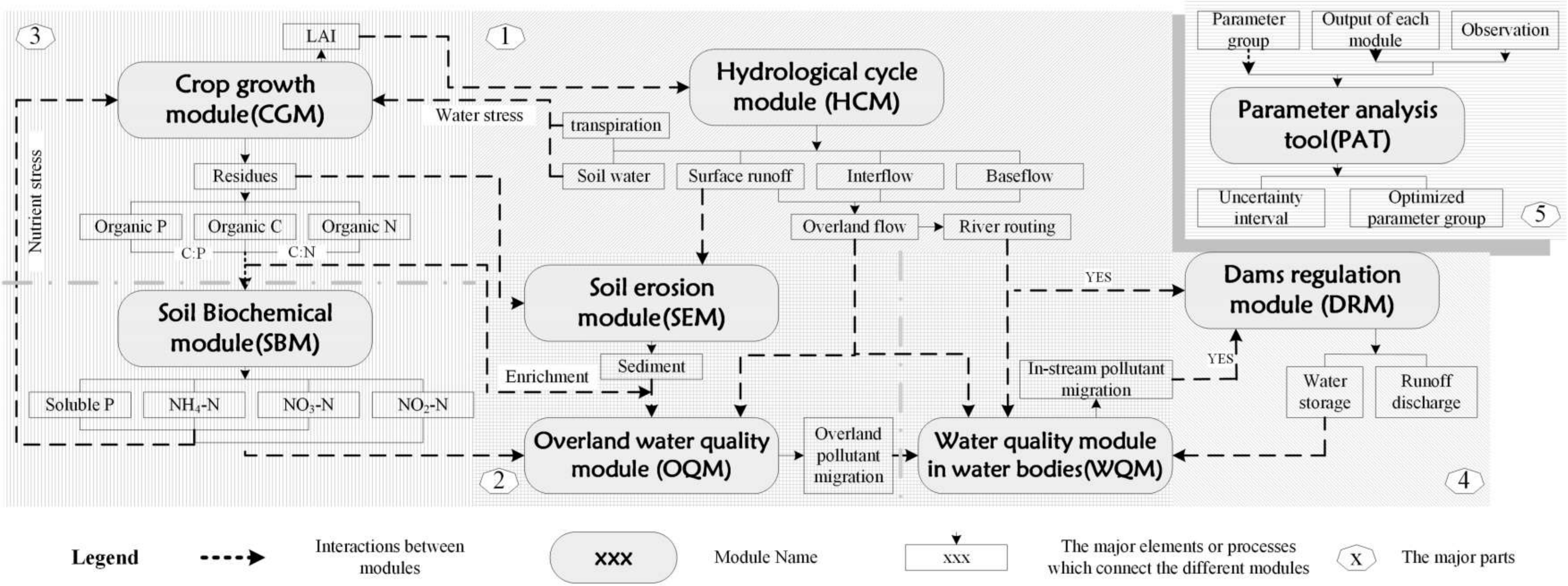

3
LAI
1
Crop growth module(CGM)
Hydrological cycle module (HCM)
Water stress
transpiration
Nutrient stress
Residues
Soil water
Surface runoff
Interflow
Baseflow
Organic P
Organic C
Organic N
Overland flow
River routing
C:P
C:N
Soil erosion module(SEM)
YES
Dams regulation module (DRM)
Soil Biochemical module(SBM)
Enrichment
Sediment
In-stream pollutant migration
YES
Water storage
Runoff discharge
Soluble P
NH4-N
NO3-N
NO2-N
Overland water quality module (OQM)
Overland pollutant migration
Water quality module in water bodies(WQM)
2
4
Parameter group
Output of each module
Observation
Parameter analysis tool(PAT)
Uncertainty interval
Optimized parameter group
5
Legend
Interactions between modules
xxx
Module Name
xxx
The major elements or processes which connect the different modules
X
The major parts

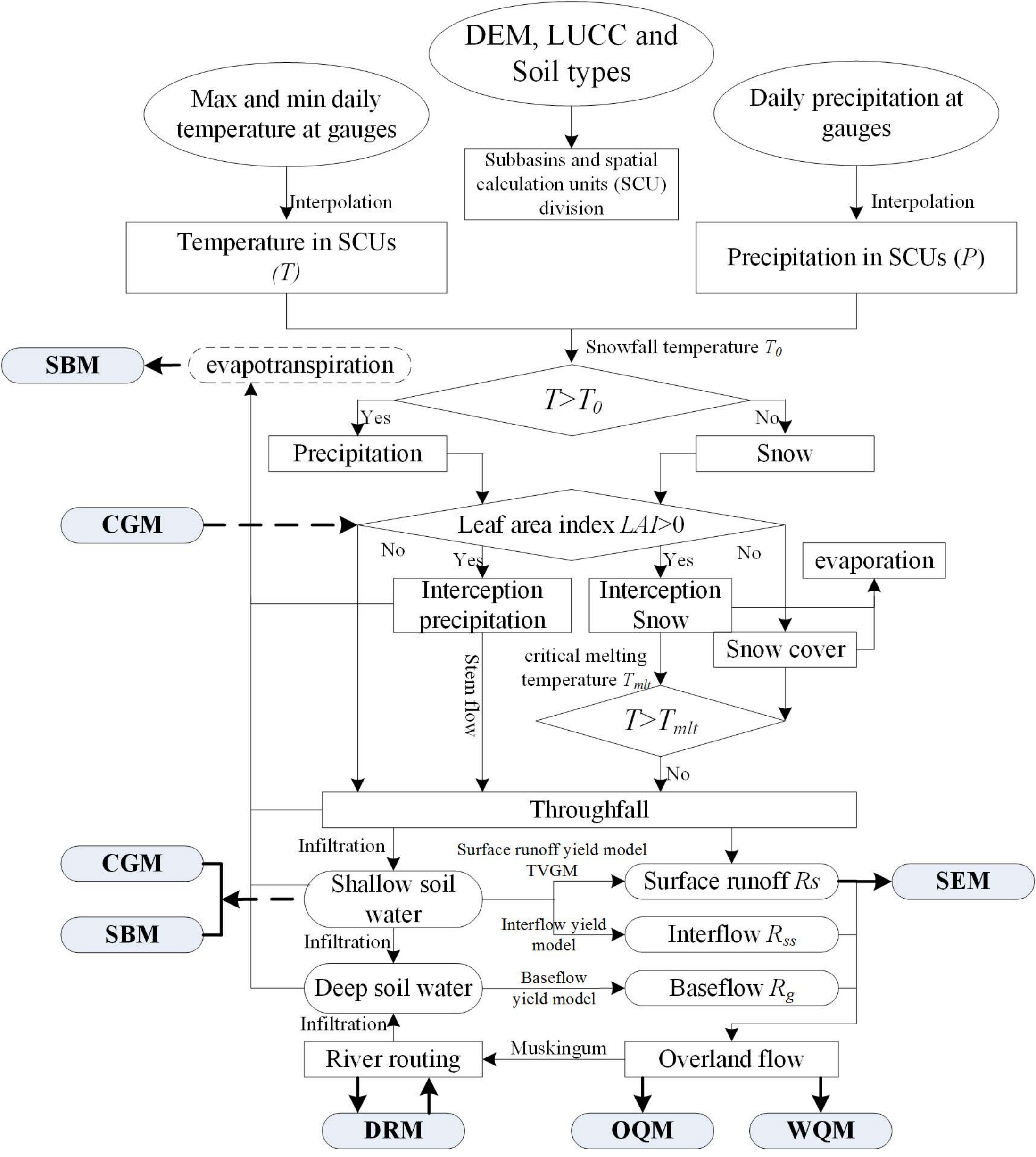

DEM, LUCC and Soil types
Max and min daily temperature at gauges
Daily precipitation at gauges
Subbasins and spatial calculation units (SCU) division
Interpolation
Interpolation
Temperature in SCUs (T)
Precipitation in SCUs (P)
Snowfall temperature T_0
SBM
evapotranspiration
$T>T_0$
Yes
No
Precipitation
Snow
CGM
Leaf area index LAI>0
No
Yes
Yes
No
evaporation
Interception precipitation
Interception Snow
Snow cover
Stem flow
critical melting temperature T_{mlt}
$T>T_{mlt}$
No
Throughfall
Infiltration
Surface runoff yield model TVGM
CGM
Shallow soil water
Surface runoff Rs
SEM
SBM
Interflow yield model
Interflow R_{ss}
Infiltration
Deep soil water
Baseflow yield model
Baseflow R_g
Infiltration
River routing
Muskingum
Overland flow
DRM
OQM
WQM

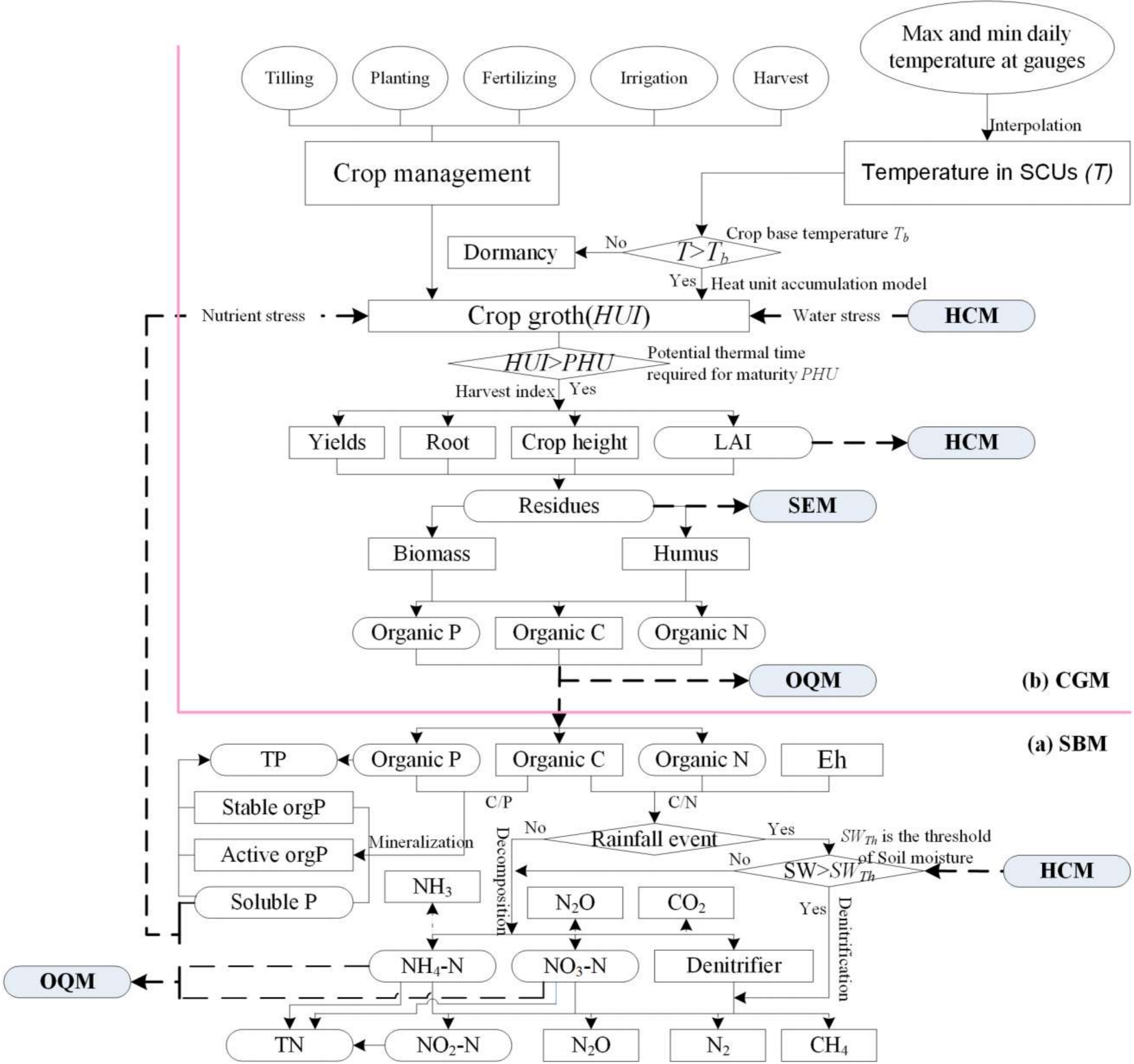

Max and min daily temperature at gauges
Tilling
Planting
Fertilizing
Irrigation
Harvest
Interpolation
Crop management
Temperature in SCUs (T)
Dormancy
No
T>Tb
Crop base temperature Tb
Yes
Heat unit accumulation model
Nutrient stress
Crop groth(HUI)
Water stress
HCM
HUI>PHU
Potential thermal time required for maturity PHU
Harvest index
Yes
Yields
Root
Crop height
LAI
HCM
Residues
SEM
Biomass
Humus
Organic P
Organic C
Organic N
OQM
(b) CGM
(a) SBM
TP
Organic P
Organic C
Organic N
Eh
Stable orgP
C/P
C/N
Active orgP
Mineralization
No
Rainfall event
Yes
SWTh is the threshold of Soil moisture
Decomposition
No
SW>SWTh
HCM
NH3
Soluble P
N2O
CO2
Yes
Denitrification
OQM
NH4-N
NO3-N
Denitrifier
TN
NO2-N
N2O
N2
CH4

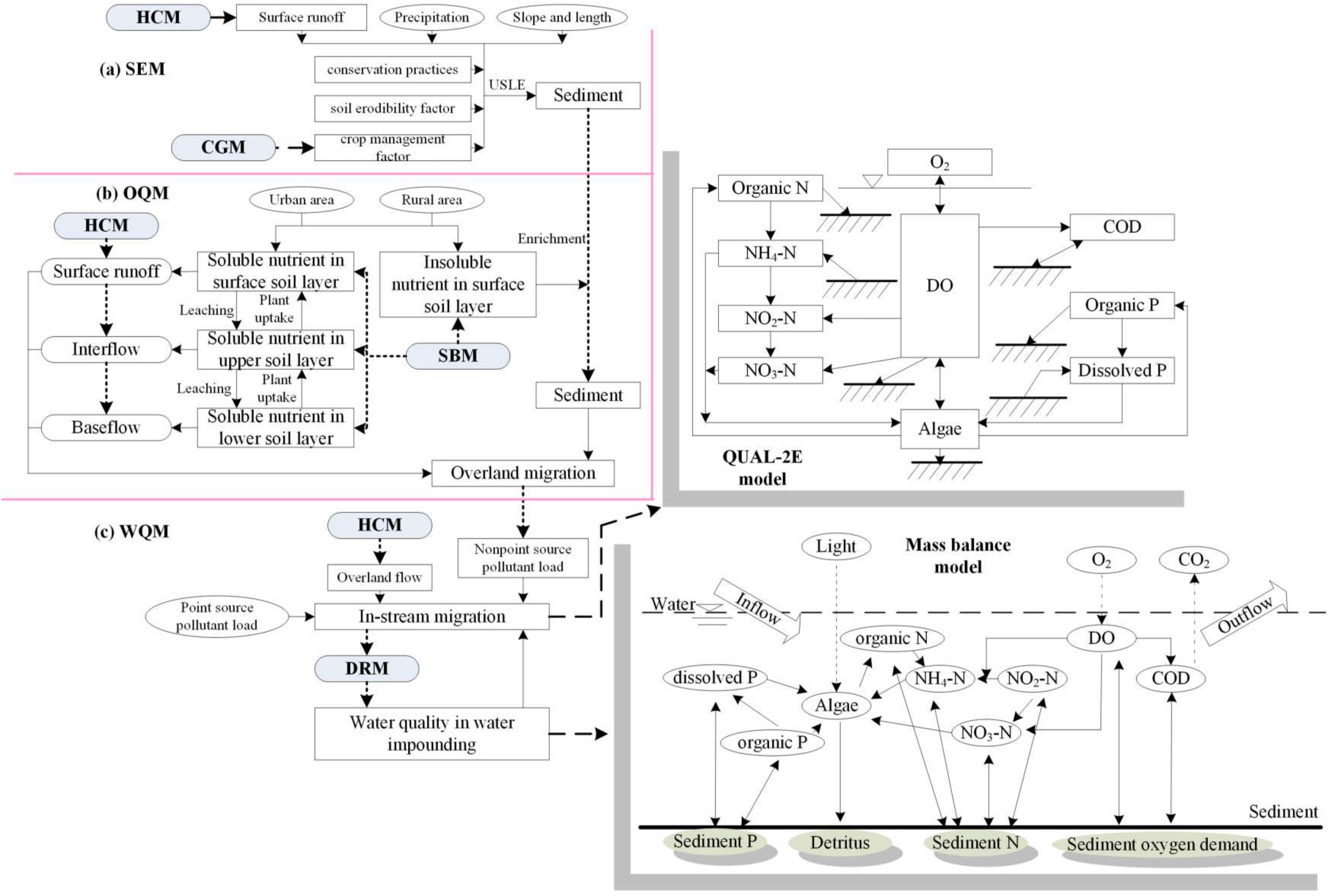

(a) SEM
HCM
Surface runoff
Precipitation
Slope and length
conservation practices
soil erodibility factor
CGM
crop management factor
USLE
Sediment
(b) OQM
Urban area
Rural area
HCM
Surface runoff
Soluble nutrient in surface soil layer
Insoluble nutrient in surface soil layer
Enrichment
Leaching
Plant uptake
Interflow
Soluble nutrient in upper soil layer
SBM
Leaching
Plant uptake
Baseflow
Soluble nutrient in lower soil layer
Sediment
Overland migration
(c) WQM
HCM
Overland flow
Nonpoint source pollutant load
Point source pollutant load
In-stream migration
DRM
Water quality in water impounding
O2
Organic N
NH4-N
NO2-N
NO3-N
DO
COD
Organic P
Dissolved P
Algae
QUAL-2E model
Light
Mass balance model
O2
CO2
Water
Inflow
Outflow
organic N
DO
dissolved P
NH4-N
NO2-N
COD
Algae
NO3-N
organic P
Sediment
Sediment P
Detritus
Sediment N
Sediment oxygen demand

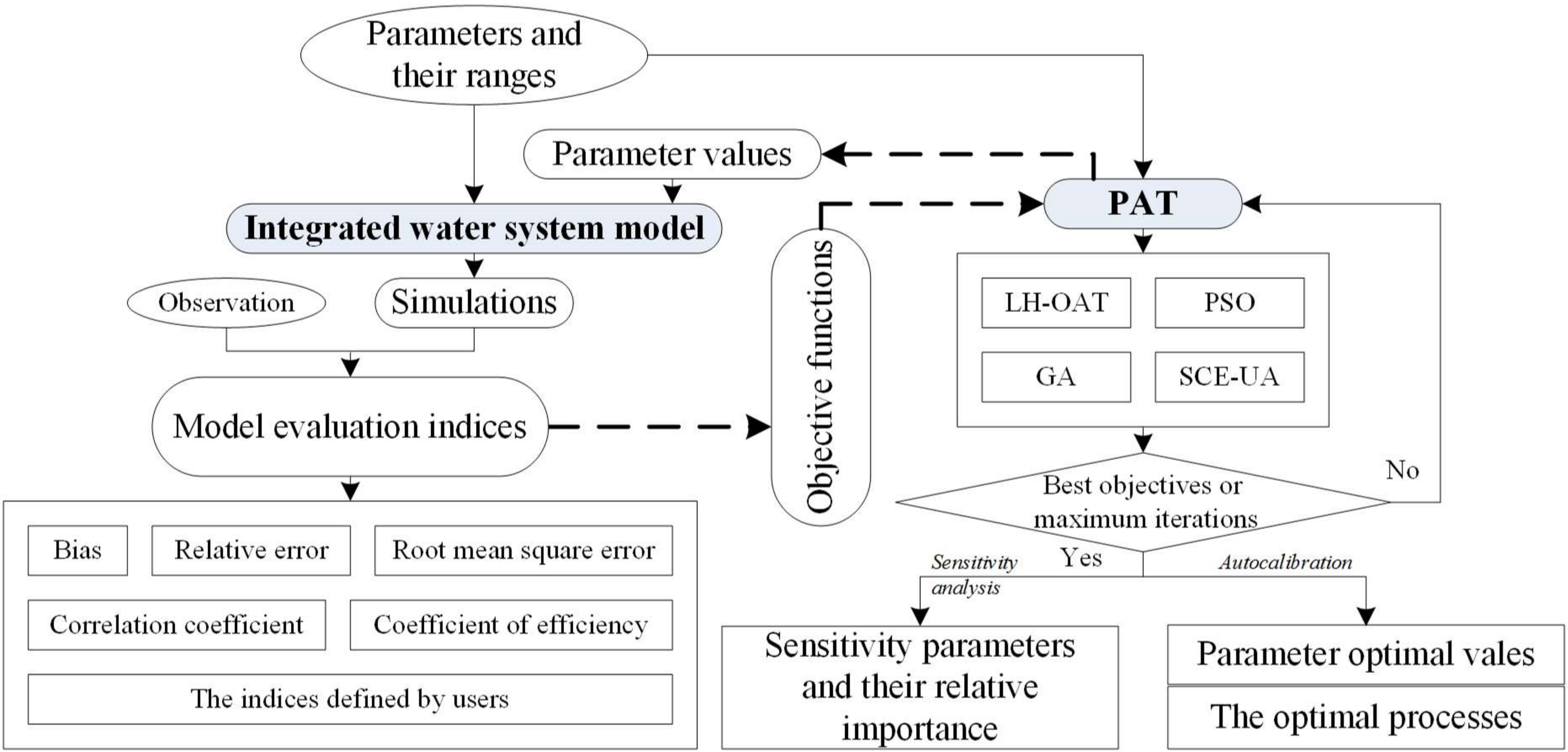

Parameters and their ranges
Parameter values
PAT
Integrated water system model
Objective functions
Observation
Simulations
LH-OAT
PSO
GA
SCE-UA
Model evaluation indices
Best objectives or maximum iterations
No
Yes
Sensitivity analysis
Autocalibration
Bias
Relative error
Root mean square error
Correlation coefficient
Coefficient of efficiency
The indices defined by users
Sensitivity parameters and their relative importance
Parameter optimal vales
The optimal processes

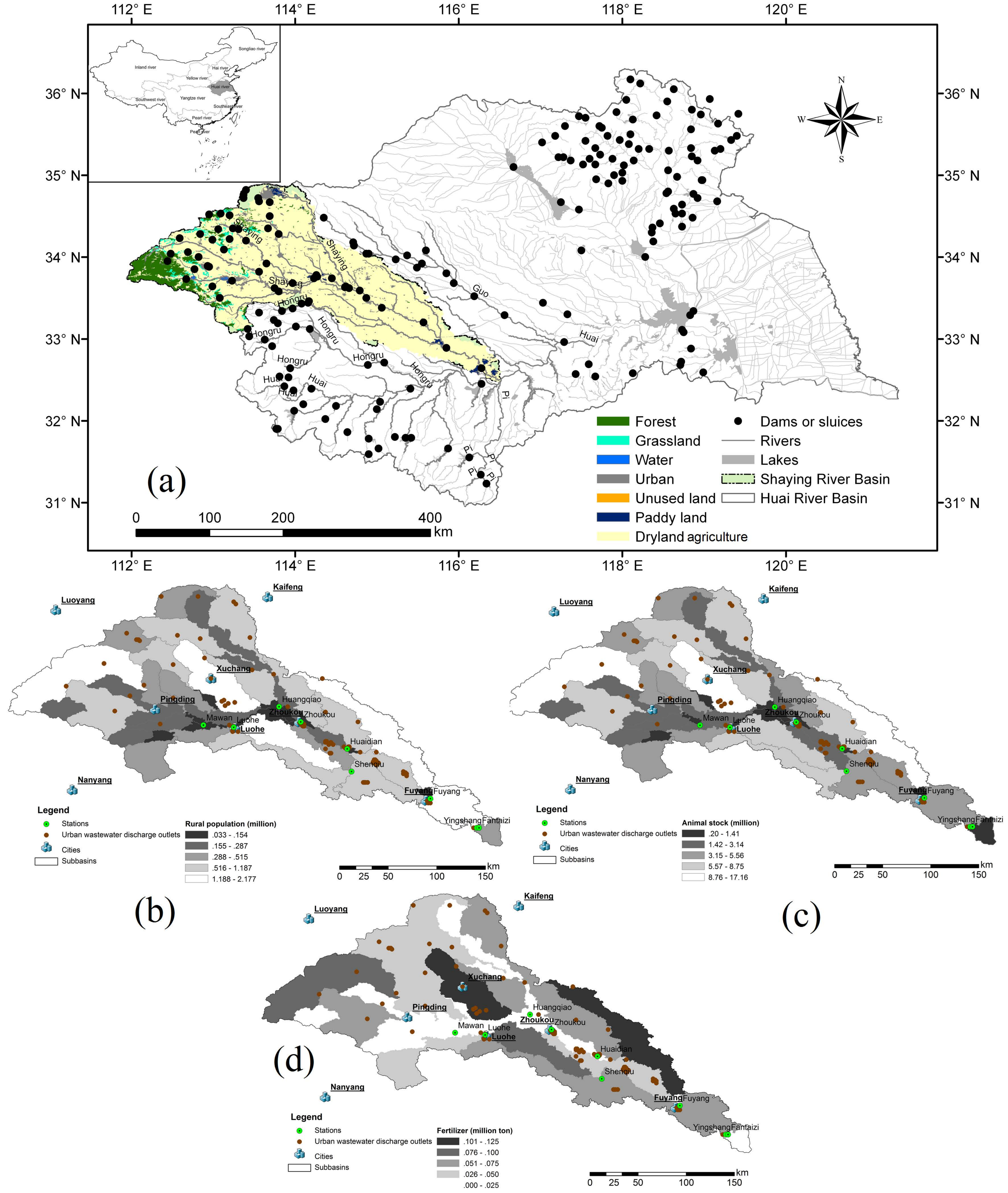
112° E
114° E
116° E
118° E
120° E
36° N
35° N
34° N
33° N
32° N
31° N
Songliao river
Inland river
Hai river
Yellow river
Huai river
Southwest river
Yangtze river
Southeast river
Pearl river
N
S
W
E
Shaying
Shaying
Shaying
Hongru
Hongru
Hongru
Hongru
Hongru
Hongru
Guo
Huai
Huai
Huai
Pi
Pi
(a)
0
100
200
400
km
Forest
Grassland
Water
Urban
Unused land
Paddy land
Dryland agriculture
Dams or sluices
Rivers
Lakes
Shaying River Basin
Huai River Basin
Luoyang
Kaifeng
Xuchang
Pingding
Huangqiao
Zhoukou
Mawan
Luohe
Huaidian
Shenqiu
Nanyang
Fuyang
Yingshang
Fantaizi
Legend
Stations
Urban wastewater discharge outlets
Cities
Subbasins
Rural population (million)
.033 - .154
.155 - .287
.288 - .515
.516 - 1.187
1.188 - 2.177
0 25 50 100 150
km
(b)
Animal stock (million)
.20 - 1.41
1.42 - 3.14
3.15 - 5.56
5.57 - 8.75
8.76 - 17.16
(c)
(d)
Fertilizer (million ton)
.101 - .125
.076 - .100
.051 - .075
.026 - .050
.000 - .025

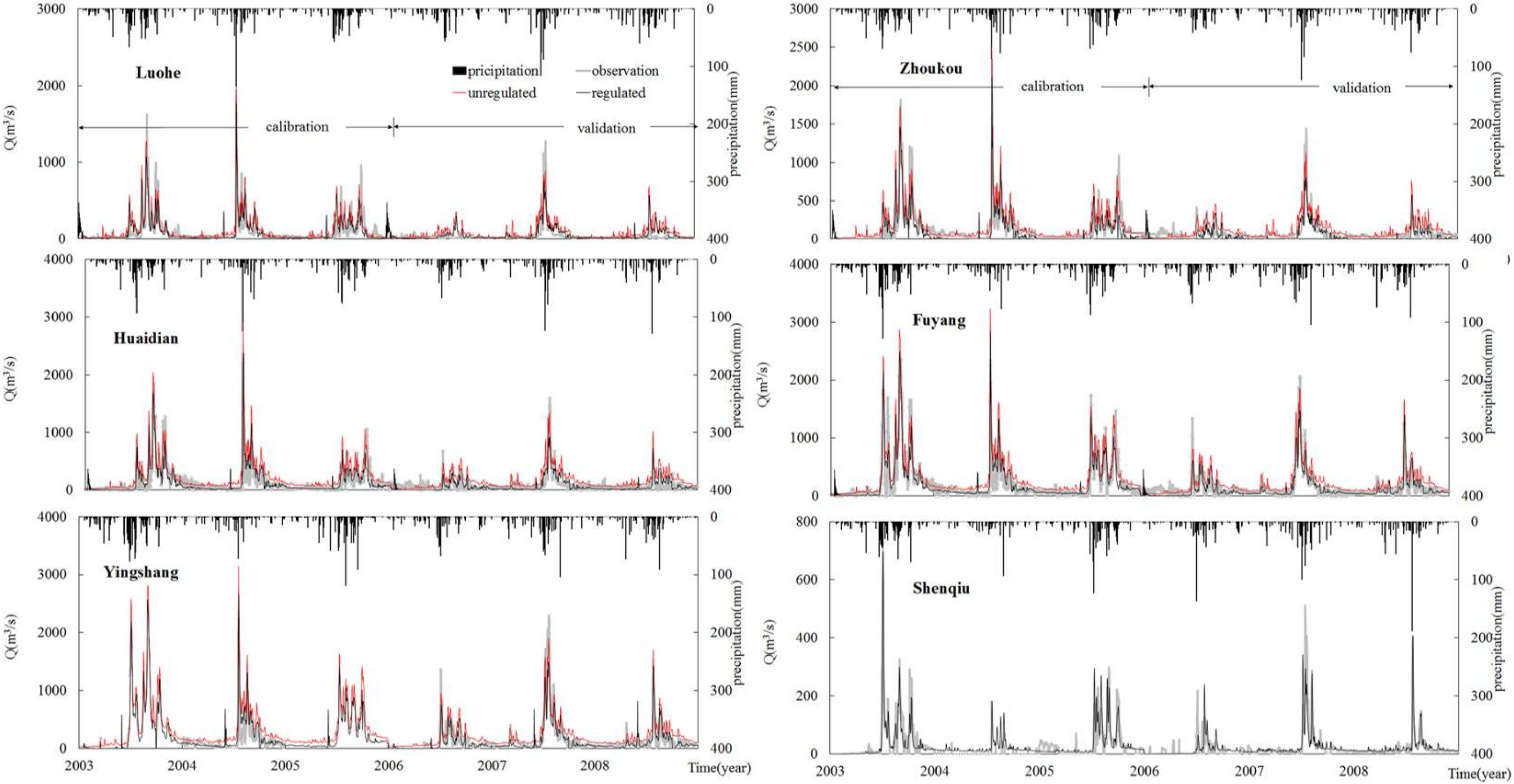

Luohe
pricipitation
observation
unregulated
regulated
calibration
validation
Huaidian
Yingshang
Zhoukou
Fuyang
Shenqiu
Q(m³/s)
precipitation(mm)
Time(year)
2003
2004
2005
2006
2007
2008

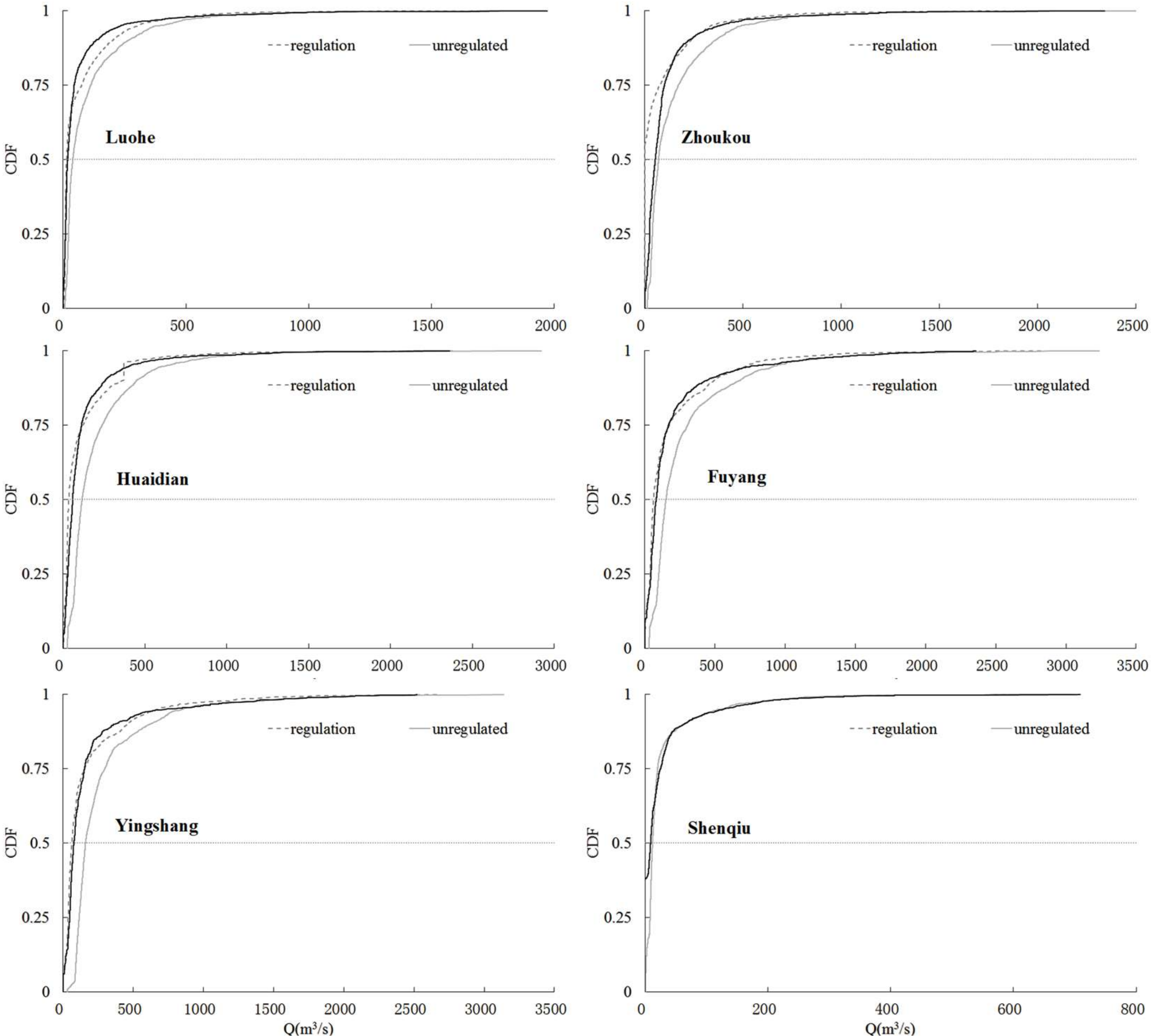
Luohe
Zhoukou
Huaidian
Fuyang
Yingshang
Shenqiu
regulation
unregulated
CDF
Q(m³/s)

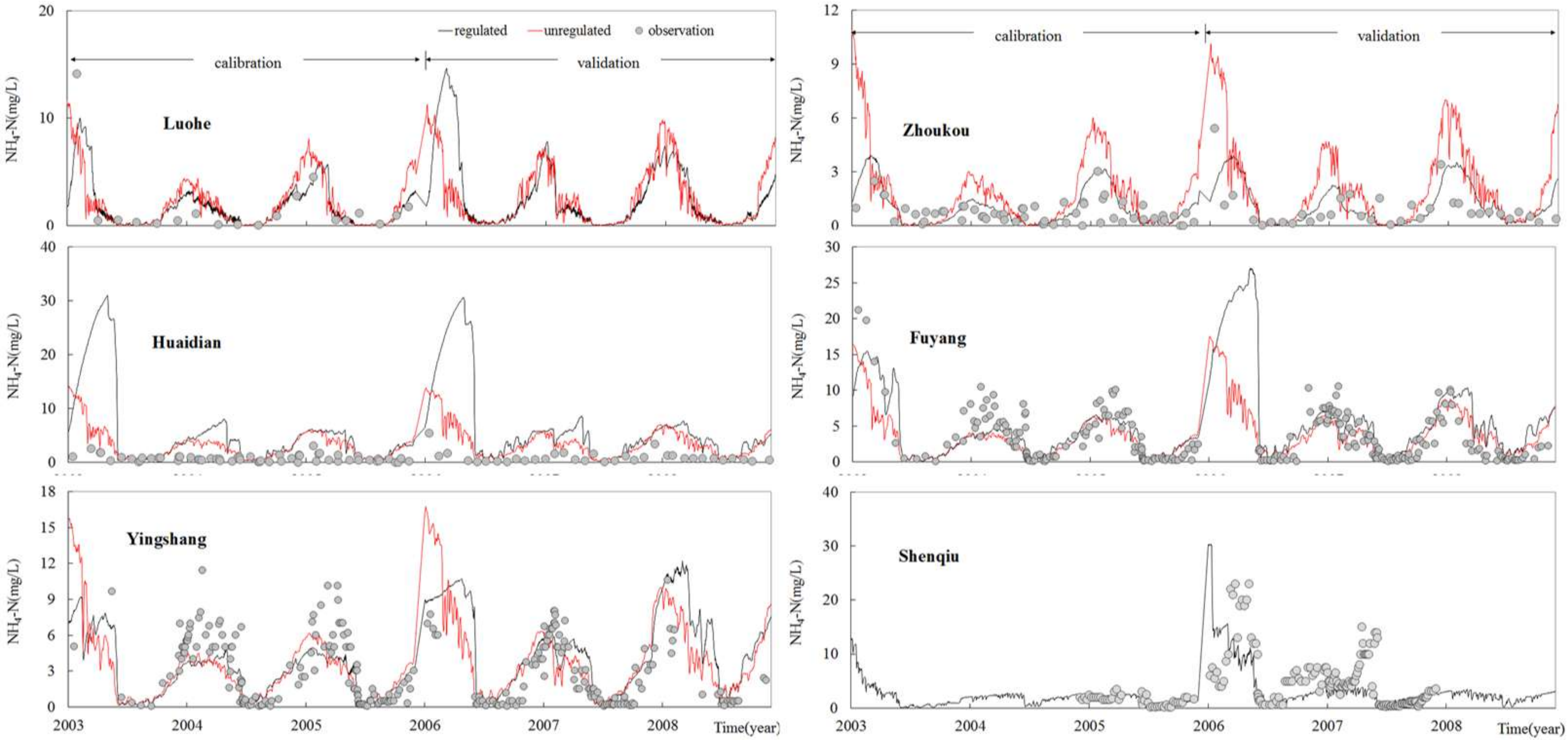

regulated
unregulated
observation
calibration
validation
Luohe
Zhoukou
Huaidian
Fuyang
Yingshang
Shenqiu
NH4-N(mg/L)
Time(year)

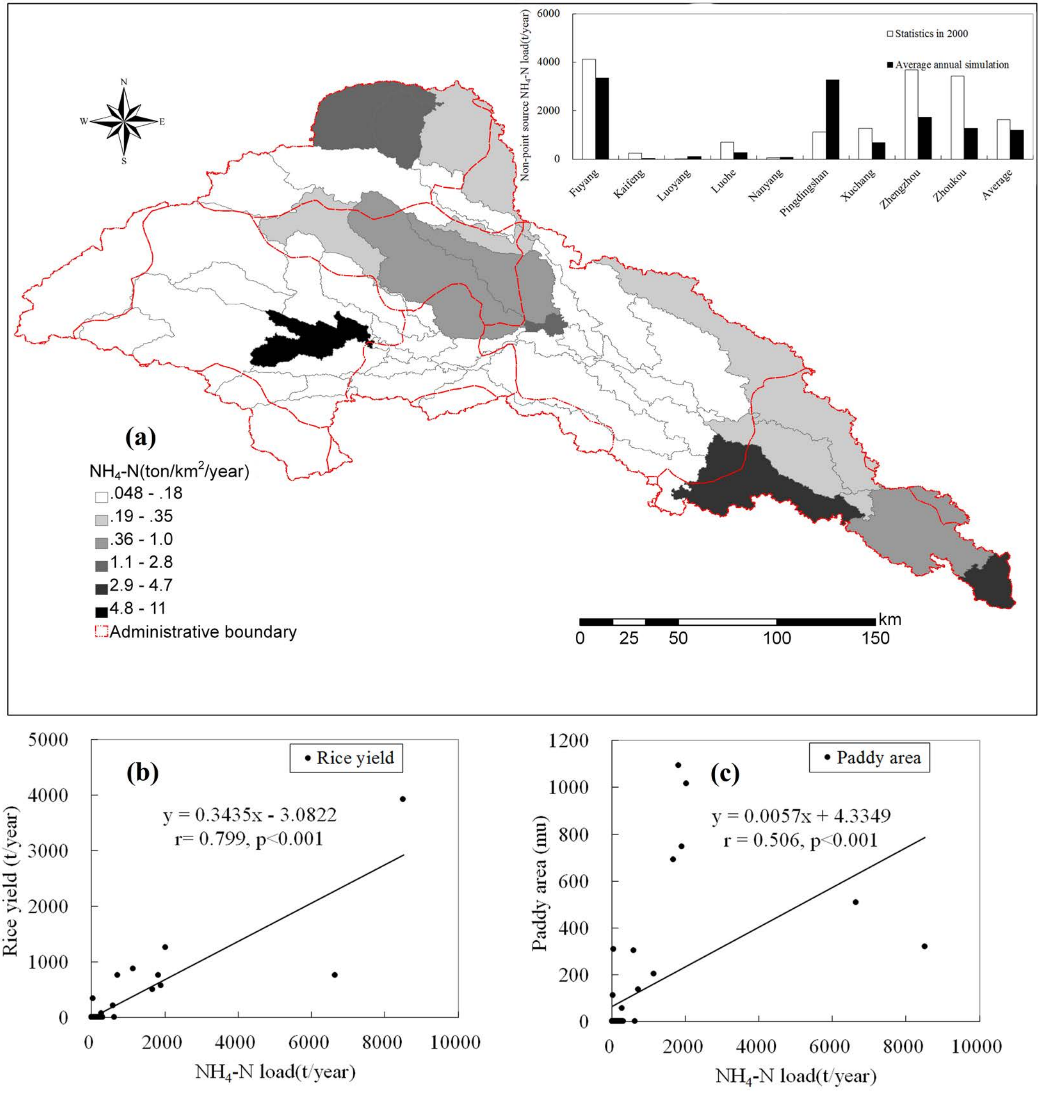

Non-point source NH4-N load(t/year)
Statistics in 2000
Average annual simulation
Fuyang
Kaifeng
Luoyang
Luohe
Nanyang
Pingdingshan
Xuchang
Zhengzhou
Zhoukou
Average
N
S
W
E
(a)
NH4-N(ton/km2/year)
.048 - .18
.19 - .35
.36 - 1.0
1.1 - 2.8
2.9 - 4.7
4.8 - 11
Administrative boundary
km
0 25 50 100 150
(b)
Rice yield
y = 0.3435x - 3.0822
r= 0.799, p<0.001
Rice yield (t/year)
NH4-N load(t/year)
(c)
Paddy area
y = 0.0057x + 4.3349
r = 0.506, p<0.001
Paddy area (mu)
NH4-N load(t/year)

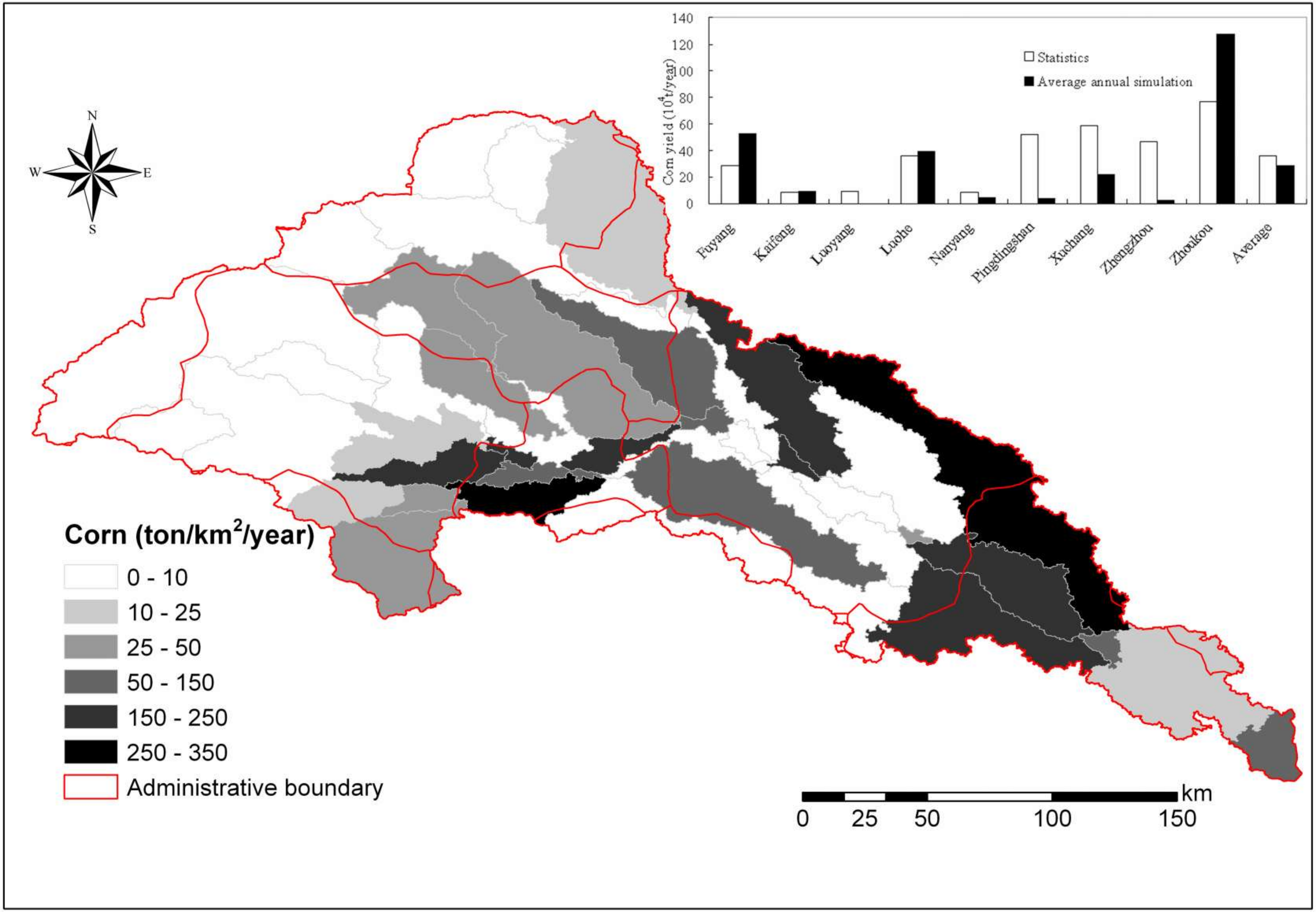

N
S
W
E
Corn (ton/km2/year)
0 - 10
10 - 25
25 - 50
50 - 150
150 - 250
250 - 350
Administrative boundary
km
0
25
50
100
150
Corn yield (10^4 t/year)
Statistics
Average annual simulation
0
20
40
60
80
100
120
140
Fuyang
Kaifeng
Luoyang
Luohe
Nanyang
Pingdingshan
Xuchang
Zhengzhou
Zhoukou
Average

Supplementary material

1. Soil P cycle simulation (Neitsch *et al.*, 2011)

Mineralization: The mineralized P is added to the solution P pool. The amounts of active and stable organic P pools ($orgP_{act}$ and $orgP_{sta}$, kg/ha) are calculated as

$$\begin{cases} orgP_{act} = orgP_{hum} \cdot orgN_{act} / (orgN_{act} + orgN_{sta}) \\ orgP_{sta} = orgP_{hum} \cdot orgN_{sta} / (orgN_{act} + orgN_{sta}) \end{cases} \quad \text{(S1)}$$

where $orgP_{hum}$ is the humic organic P amount (kg/ha); $orgN_{act}$ and $orgN_{sta}$ are the amounts of N in the active organic pool and stable organic pool (kg/ha), respectively, which are simulated by DNDC.

The mineralization rate of the humus active organic P pool (RHP) is calculated by

$$RHP = 1.4 \cdot \beta_{\min} \cdot (\gamma_{tmp} \cdot \gamma_{SW})^{1/2} \quad \text{(S2)}$$

where β_{min} is the mineralization rate of the humus active organic P; γ_{tmp} and γ_{SW} are the reduction factors of soil temperature and moisture.

The mineralization rate of the residue fresh organic P pool (RRP) is calculated as

$$RRP = 0.8 \cdot \delta_P = 0.8 \cdot \beta_{rsd} \cdot \gamma_P \cdot (\gamma_{tmp} \cdot \gamma_{SW})^{1/2} \quad \text{(S3)}$$

where δ_P and β_{rsd} are the residue decay rate and the mineralization rate of the residue fresh organic P. γ_P is the P cycling residue composition factor.

Decomposition: The decomposition rate of the residue fresh organic P pool (DRP) is

$$DRP = 0.2 \cdot \delta_P \quad \text{(S4)}$$

Sorption: The P movement between the soluble and active mineral pools ($P_{sol|act}$, kg/ha) and between active and stable mineral pools ($P_{act|sta}$, kg/ha) are

$$P_{sol|act} = \begin{cases} P_{sol} - \min P_{act} \cdot pai/(1-pai) & if \quad P_{sol} > \min P_{act} \cdot pai/(1-pai) \\ 0.1 \cdot [P_{sol} - \min P_{act} \cdot pai/(1-pai)] & if \quad P_{sol} < \min P_{act} \cdot pai/(1-pai) \end{cases} \quad \text{(S5)}$$

and

$$P_{act|sta} = \begin{cases} 0.0006 \cdot (4 \cdot \min P_{act} - \min P_{sta}) & if \quad \min P_{sta} < 4 \cdot \min P_{act} \\ 0.00006 \cdot \beta_{eqP} \cdot (4 \cdot \min P_{act} - \min P_{sta}) & if \quad \min P_{sta} > 4 \cdot \min P_{act} \end{cases} \quad \text{(S6)}$$

respectively. Where P_{sol}, $minP_{act}$ and $minP_{sta}$ are the amounts of soluble, mineral active and stable P (kg/ha), respectively; *pai* is P availability index.

2. Crop growth module

2.1 Crop yield (Williams *et al.*, 1989)

The crop growth depends on the accumulation of thermal time (Sharpley and Williams, 1990). The daily thermal time (HU, °C) and the thermal time index for j^{th} crop (HUI) are calculated as:

$$\begin{cases} HU_K = (T_{mx,K} + T_{mn,K})/2 - T_{b,j} \\ HUI_i = \sum_{K=1}^{i} HU_K \Big/ PHU_j \end{cases} \tag{S7}$$

where $T_{mx,K}$ and $T_{mn,K}$ are the maximum and minimum temperatures (°C) on the K^{th} day, respectively; $T_{b,j}$ is the base temperature of the j^{th} crop (°C). Crop growth will stop when HU_K is below 0.0. PHU_j is the required cumulative thermal time for the j^{th} crop from sowing to physical maturity (°C). The range of HUI is from 0.0 at sowing to 1.0 at maturity. i is the total days of crop growth.

The daily potential biomass accumulation (ΔB_p, t/ha/d) is estimated as follow:

$$\begin{aligned} \Delta B_{p,i} &= 0.001 \cdot BE_i \cdot PAR_i \cdot [1 + \Delta HRLT_i]^3 \\ &= 0.0005 \cdot BE_i \cdot RA_i \cdot [1 - \exp(-0.65 \cdot LAI)] \cdot [1 + \Delta HRLT_i]^3 \end{aligned} \tag{S8}$$

where BE is the crop parameter for converting energy to biomass (kg·ha·m^2/MJ); $HRLT$ and $\Delta HRLT$ are length of a day (hr) and its variation (hr/d), respectively; PAR is intercepted photosynthetic active radiation (MJ/m^2). RA is solar radiation (MJ/m^2) and LAI is leaf area index (m^2/m^2), which is a function of heat units, crop stress and crop development stages.

From emergence to the start of leaf decline, LAI is estimated with the equation:

$$\begin{aligned} LAI_i &= LAI_{i-1} + \Delta LAI \\ &= LAI_{i-1} + (\Delta HUF)(LAI_{mx})(1 - \exp(5 \cdot (LAI_{i-1} - LAI_{mx}))) \cdot \sqrt{REG_i} \end{aligned} \tag{S9}$$

From the start of leaf decline to the end of the growing season,

$$LAI_i = LAI_0 \cdot (1 - HUI_i / 1 - HUI_0)^{ad_j} \tag{S10}$$

where *HUF* is a thermal time factor; *REG* is minimum crop stress factor; *Ad* is a parameter controlled *LAI* decline rate for crop *j*; HUI_0 is the *HUI* value when *LAI* begins to decline.

The biomass accumulation is constrained by the stresses of soil water, temperature, nutrient (N and P) and aeration conditions.

$$\Delta B = \Delta B_p \cdot REG = \Delta B_p \cdot \min(WS, TS, SN, SP, AS) \tag{S11}$$

where *REG* is the crop growth regulating factor.

The water stress: $$WS_i = \sum_{l=1}^{M} U_{l,i} \Big/ E_{P,i} \tag{S12}$$

The temperature stress: $$TS_i = \sin[\pi \cdot (T_{g,i} - T_{b,j})/2(T_{o,j} - T_{b,j})] \quad 0 \le TS_i \le 1 \tag{S13}$$

The N stress: $$\begin{cases} SN_{S,i} = 2[1 - \sum_{K=1}^{i} UN_K \Big/ (c_{NB,i} \cdot B_i)] \\ SN_i = 1 - SN_{S,i}/[SN_{S,i} + \exp(3.39 - 10.93 SN_{S,i})] \end{cases} \tag{S14}$$

The P stress: $$\begin{cases} SP_{S,i} = 2[1 - \sum_{K=1}^{i} UP_K \Big/ (c_{NP,i} \cdot B_i)] \\ SP_i = 1 - SP_{S,i}/[SP_{S,i} + \exp(3.39 - 10.93 SP_{S,i})] \end{cases} \tag{S15}$$

The aeration stress: $$\begin{cases} SAT = SW1/PO1 - CAF_j \\ AS_{S,i} = 1 - SAT/[SAT + \exp(-1.291 - 56.1 \cdot SAT)] \quad SAT > 0.0 \end{cases}$$

(S16)

where T_g and T_0 are the average daily soil surface temperature and the optimal temperature (°C) for crop *j*, respectively; *SAT* is the saturated soil moisture (mm/mm); *SW1* and *PO1* are the soil moisture (mm/mm) and porosity of the top 1m of soil, respectively; *CAF* is critical aeration factor for crop *j*; *AS* is aeration stress factor.

The crop yield (*YLD*, t/ha) is estimated using the harvest index, viz.:

$$YLD_j = HI_j \cdot B_{AG} \tag{S17}$$

where *HI* is harvest index for cop j; B_{AG} is the above-ground biomass (t/ha)..

2.2 Water use

The daily potential water use from surface soil to any root depth is calculated as

$$U_{p,i} = E_{p,i} \cdot [1 - \exp(-\Lambda \cdot Z/RZ)]/[1 - \exp(-\Lambda)] \quad \text{(S18)}$$

The potential water use ($U_{p,l}$, mm/day) in layer l is calculated by taking the difference between $U_{p,i}$ values at the layer boundaries, viz.,

$$U_{p,l} = E_{p,i} \cdot \left[\exp(-\Lambda \cdot Z_{l-1}/RZ) - \exp(-\Lambda \cdot Z_l/RZ)\right]/[1 - \exp(-\Lambda)] \quad \text{(S19)}$$

where $U_{p,i}$ is the total water used to depth Z m on day i (mm); RZ is the root zone depth (m); Λ is a water use distribution parameter.

Restricted by soil moisture, the water use ($U_{l,i}$, mm/day) in layer l on day i is calculated with the following equations (Jones and Kiniry, 1986).

$$U_{l,i} = \begin{cases} U_{p,l} \cdot \exp\left[20 \cdot (SW_{l,i} - WP_l)/(FC_l - WP_l) - 1\right] & if\ SW_{l,i} < (FC_l - WP)_l/4 + WP_l \\ U_{p,l} & if\ SW_l \geq (FC_l - WP_l)/4 + WP_l \end{cases}$$

(S20)

2.3 Nutrient uptake

The daily crop nutrient (N and P) demands are the differences between crop nutrient demands and potential nutrient contents.

$$\begin{cases} UND_i = c_{NB,i} \cdot B_i - \sum_{K=1}^{i} UN_K \\ UPD_i = c_{PB,i} \cdot B_i - \sum_{K=1}^{i} UP_K \end{cases} \quad \text{(S21)}$$

where UND and UNP are the potential daily N and P demands, respectively (kg/ha); UN and UP are the actual uptakes of N and P, respectively (kg/ha); c_{NB} and c_{NP} are the optimal N and P concentrations of the crop, rescpetively (kg/t); B is the daily biomass accumulation (t/ha).

The actual soluble N (NO_3-N and NH_4-N) mass uptaken by crops is calculated as.

$$\begin{cases} UN_{l,i} = U_{l,i} \cdot (WN_l/SW_l)_i \\ UNS_i = \sum_{K=1}^{M} UN_{l,i} \end{cases} \quad \text{(S22)}$$

where $UN_{l,i}$ is the actual uptakes of N in the layer l on day i. WN is NO_3^-N or NH_4-N amount in the soil (kg/ha). The amount of N supplied by soil (UNS) is estimated by summing UN of all layers (kg/ha).

The soil P availability is calculated as.

$$\begin{cases} UPS_i = 1.50 \cdot UPD_i \cdot \sum_{l=1}^{M} LF_{u,l} \cdot (RW_l / RWT_i) \\ LF_{u,l} = 0.1 + 0.9 \cdot c_{LP,l} / [c_{LP,l} + 117 \cdot \exp(-0.283 \cdot c_{LP,l})] \end{cases} \quad (S23)$$

where UPS is the amount of P supplied by soil (kg/ha); RW and RWT are the root weights in layer l and in total, rescpetively (kg/ha); LF_u is the labile P factor for uptake (g/t).

A portion of uptake N will be fixed by legumes, viz.,

$$\begin{cases} WFX_i = FXR_i \cdot UND_i & WFX \le 6.0 \\ FXR = \min(1.0, FXW, FXN) \cdot FXG \end{cases} \quad (S24)$$

where FXG is the growth stage factor; FXW and FXN are the factors of soil water and NO_3-N, respectively. All of these factors are calculated using the follow equations.

$$FXG_i = \begin{cases} 0.0 & HUI_i \le 0.15, HUI_i \ge 0.75 \\ 6.67 HUI_i - 1.0 & 0.15 < HUI_i \le 0.3 \\ 1.0 & 0.3 < HUI_i \le 0.55 \\ 3.75 - 5.0 HUI_i & 0.55 < HUI_i < 0.75 \end{cases} \quad (S25)$$

$$FXW_i = (SW_{0.3,i} - WP_{0.3}) / 0.85 \cdot (FC_{0.3} - WP_{0.3}) \quad SW_{0.3} < 0.85(FC_{0.3} - WP_{0.3}) + WP_{0.3} \quad (S26)$$

$$FXN_i = \begin{cases} 0.0 & WNO_3 > 300 kg \cdot ha^{-1} \cdot m^{-1} \\ 1.5 - 0.005 \cdot WNO_3 / RD & 100 < WNO_3 \le 300 \\ 1.0 & WNO_3 \le 100 \end{cases} \quad (S27)$$

where $SW_{0.3}$, $WP_{0.3}$ and $FC_{0.3}$ are the moisture in the top 0.3 m soil, at wilting point and field capacity (mm), respectively.

3. Soil erosion module (Onstad and Foster, 1975)

The soil erosion by precipitation is estimated using the improved USLE equation (Onstad and Foster, 1975), viz.,

$$Y = \begin{cases} (0.646 EI + 0.45 Q \cdot q_p^{0.333}) \cdot K \cdot CE \cdot PE \cdot LS & Q > 0. \\ 0 & Q = 0. \end{cases} \quad (S28)$$

where Y is the sediment yield (t/ha); Q is the runoff depth (mm); q_p is the peak runoff rate (mm/hr); K is the soil erodibility factor determined by the soil type; PE is the erosion control practice factor.

LS is the factor of slope length and steepness:

$$\begin{cases} LS = (\lambda/22.1)^{\xi}(65.41S^2 + 4.56S + 0.065) \\ \xi = 0.6 \cdot [1 - \exp(-35.835S)] \end{cases} \tag{S29}$$

CE is the crop management factor:

$$CE = (0.8 - CE_{mn,j})\exp(-0.00115CV) + CE_{mn,j} \tag{S30}$$

EI is the precipitation energy factor:

$$EI = P \cdot [12.1 + 8.9 \cdot (\log r_p - 0.434) \cdot r_{0.5}]/1000 \tag{S31}$$

where S and λ are the land surface slope (m/m) and slope length (m), both of which are obtained during the procedure of preparing the spatial simulation units; ζ is a parameter dependent upon slope; $CE_{mn,j}$ is the minimum crop management factor of crop j; CV is soil cover (above ground biomass and residue) (kg/ha); P is the daily precipitation (mm); r_p, $r_{0.5}$ is the peak precipitation rate and maximum 0.5 h precipitation intensity (mm/hr). The value of r_p is obtained according to the exponential precipitation distribution.

4. Overland water quality module

4.1 Nutrient loss in urban and rural area

Generally, the inhabitant and industrial sewage in the urban area are collected, treated and discharged into river system from the wastewater discharge outlets. This amount of nutrient flux is the model input as the point source pollutant load. The nonpoint source nutrient loss in urban area takes place along the overland flow and is estimated using the export coefficient model (Johnes, 1996).

$$V_{ur\_N} = 100 \cdot c_{ur\_N} \cdot Area_{urban} \tag{S32}$$

where V_{ur_N}, c_{ur_N} and $Area_{urban}$ are the amount of nutrient loss in the urban area (kg); the export coefficient (kg/ha/year) and urban area (km^2), respectively.

The farm manure of rural living and livestock farming is also considered as one of important nonpoint source of nutrient due to the deficiency of sewage treatment facilities in the rural area. The total loss is estimated as.

$$\begin{cases} V_{liv\_N} = c_{liv\_N} \cdot Pop_{rural} \\ V_{lst\_N} = c_{lst\_N} \cdot Pop_{stock} \end{cases} \qquad \text{(S33)}$$

where V_{liv_N} and V_{lst_N} are the amounts of nutrient loss from living and livestock farming in the rural area, respectively (kg/year). C_{liv_N} and C_{lst_N} are the export coefficients of living (kg/day/person) and livestock (kg/day/animal), respectively; Pop_{rural} and Pop_{stock} are the population and the animal stock, respectively.

4.2 Nutrient loss of soil layer

The loss of soluble nutrient is considered to happen in both upper and lower soil layers. The loss weights of NO_3^-N, NH_4-N and soluble P are calculated using the equations (Williams *et al.*, 1989), respectively.

$$\begin{cases} V_{N\_up} = W_{N\_up} \cdot [1 - \exp(-\dfrac{R_s + R_{ss}}{UL})] \\ V_{N\_low} = W_{N\_low} \cdot [1 - \exp(-\dfrac{R_{bs}}{UL})] \end{cases} \qquad \text{(S34)}$$

where W_{N_up} and W_{N_low} are the soluble nutrient weights in the upper and lower soil layers, respectively (kg/ha); UL is the maximum soil moisture (mm); V_{N_up} and V_{N_low} is the soluble nutrient loss in the upper and lower soil layers, respectively (kg/ha); Rs, Rss and Rbs are the surface runoff, interflow and baseflow(mm), respectively, which are obtained from the hydrological cycle module.

The amount of insoluble nutrients migrated with the sediment is estimated using the equation (Neitsch *et al.*, 2011)

$$Y_{ON} = 0.001 \cdot Y \cdot c_{ON} \cdot ER \qquad \text{(S35)}$$

where Y_{ON} is loss of organic N or P (kg/ha); c_{ON} is the insoluble nutrient concentration in the soil layer (g/m^3); ER is enrich ratio.

4.3 Overland migration (Neitsch *et al.*, 2011)

$$N_{overl,i} = (N'_{overl,i} + N_{stor,i-1}) \cdot [1 - \exp(-T_{retain}/T_{route})] \quad \text{(S36)}$$

where $N_{overl,i}$ is the amount of overland pollutant discharged into river system on day i including sediment (tons/day), soluble and insoluble nutrient (kg/day); $N'_{overl,i}$ and $N_{stor,i}$ are pollutant loads generated in the sub-basin on day i, retained from the previous day (tons for sediment, kg for nutrient), respectively. T_{retain} and T_{route} are the retain time and routing time of flow (days), respectively.

5. Water quality module of water bodies

The basic equation of in-stream water quality module (Brown and Barnwell 1987) is

$$dC/dt = -(R_d + R_{set}) \cdot C + \sum S_{out} \quad \text{(S37)}$$

where C is the water quality concentration (mg/L); K_d and K_{set} are the degradation and settling coefficient of pollutant (day^{-1}), respectively; and $\sum S_{out}$ is the external source items (mg/L/day).

The equation of water quality module of water impounding is as follow.

$$\begin{cases} dh/dt = [Q_{in} - Q_{out}]/A + P - E \\ dC_L/dt = [C_{in}Q_{in} - C_L Q_{out}]/Ah - K_{set}C_L - K_d C_L + K_{scu}C_s \cdot d/h \\ dC_s/dt = h/d \cdot K_{set}C_L - K_{scu}C_s - K_{bur}C_s \end{cases} \quad \text{(S38)}$$

where h and d are water and sediment depths (m), respectively; Q_{in} and Q_{out} are inflow and outflow (m^3/s), respectively; C_{in} , C_{out} , C_L and C_s are water quality concentrations into and out of the water body, in the water body and the sediment (mg/L), respectively; P and E are precipitation and evapotranspiration (m/s); K_{scu} and K_{bur} are the resuspension and decay coefficients of pollutant in the sediment (day^{-1}), respectively; A is water surface area (km^2).

Table S1. All the parameters in the extended model

ID	Variables	Definition	Unit	Affected components
Sub-basin parameters				
1	W_m	Minimum soil moisture	none	flow
2	Ww	Soil moisture at permanent wilting point	none	flow
3	W_{fc}	Field capacity of soil	none	flow
4	$W_{sat,u}$	Saturated moisture capacity of upper soil layer	none	flow
5	$W_{sat,l}$	Saturated moisture capacity of lower soil layer	none	flow
6	g_1	Basic surface runoff coefficient	none	flow
7	g_2	Influence coefficient of soil moisture	none	flow
8	K_{ET}	Adjustment factor of evapotranspiration	none	flow
9	K_{ss}	Interflow yield coefficient	none	flow
10	T_g	Delay time for aquifer recharge	day	flow
11	K_{bs}	Baseflow yield coefficient	none	flow
12	K_{sat}	Steady state infiltration rate of soil	mm/hr	flow
13	kf_{mx}	Ratio of state infiltration rate to maximum rate in soil	none	flow
14	*DtoW*	Ratio of width to depth of channel	none	flow
15	*rch_k*	Infiltration rate of channel	mm/hr	sediment
16	*ch_cov*	Channel cover factor	none	sediment
17	*ch_erod*	Channel erodibility factor	cm/hr/Pa	sediment
18	R_{set}(algae)	Settling rate of Algae at 20 ^{0}C	mg/day	algae
19	R_{set}(solP)	Settling rate of soluble P at 20 ^{0}C	mg/m^2/day	P
20	$R_{set}(NH_4)$	Settling rate of NH_4-N at 20 ^{0}C in channel	mg/m^2/day	N
21	R_{set}(orgN)	Settling rate of organic N at 20 ^{0}C in channel	day^{-1}	N
22	R_{set}(orgP)	Settling rate of organic P at 20 ^{0}C in channel	day^{-1}	P
23	R_d(COD)	COD deoxygenation rate at 20 ^{0}C in channel	day^{-1}	COD
24	Rch_k_1	Reaeration coefficients at 20 ^{0}C in channel	day^{-1}	DO
25	R_{set}(COD)	Settling rate of COD at 20 ^{0}C in channel	day^{-1}	COD
26	Rch_k_2	DO adsorption rate of sediment at 20 ^{0}C in channel	day^{-1}	DO
27	$R_d(NH_4)$	Bio-oxidation rate of NH_4-N at 20 ^{0}C in channel	day^{-1}	N
28	$R_d(NO_2)$	Oxidation rate of NO_2-N to NO_3-N at 20 ^{0}C in channel	day^{-1}	N
29	R_d(orgN)	Hydrolysis rate of organic N to NH_4-N at 20 ^{0}C in channel	day^{-1}	N
30	R_d(orgP)	Hydrolysis rate of organic P to soluble P at 20 ^{0}C in channel	day^{-1}	N
31	*CtoB*	Relationship between COD and BOD	none	COD
32	*res_k*	Infiltration rate in reservoir or sluice	mm/hr	flow
33	K_{set}(COD)	Settling rate of COD at 20 ^{0}C in reservoir or sluice	m/year	COD
34	$K_{set}(NH_4)$	Settling rate of NH_4-N at 20 ^{0}C in reservoir or sluice	m/year	N
35	$K_{set}(NO_2)$	Settling rate of NO_2-N at 20 ^{0}C in reservoir or sluice	m/year	N
36	$K_{set}(NO_3)$	Settling rate of NO_3-N at 20 ^{0}C in reservoir or sluice	m/year	N
37	K_{set}(orgN)	Settling rate of organic N at 20 ^{0}C in reservoir or sluice	m/year	N
38	K_{set}(orgP)	Settling rate of organic P at 20 ^{0}C in reservoir or sluice	m/year	P

39	K_{set}(solP)	Settling rate of soluble P at 20 ^{0}C in reservoir or sluice	m/year	P
40	K_{set} (DO)	Settling rate of DO at 20 ^{0}C in reservoir or sluice	m/year	DO
41	K_{set}(algae)	Settling rate of algae at 20 ^{0}C in reservoir or sluice	m/year	algae
42	K_{set}(TN)	Settling rate of TN at 20 ^{0}C in reservoir or sluice	m/year	N
43	K_{set}(TP)	Settling rate of TP at 20 0C in reservoir or sluice	m/year	P
44	K_d(COD)	COD deoxygenation rate in reservoirs at 20 ^{0}C	day^{-1}	COD
45	*res_k1*	Reaeration coefficients at 20 ^{0}C in reservoir or sluice	day^{-1}	DO
46	K_d(NH_4)	Bio-oxidation rate of NH_4-N in reservoir at 20 ^{0}C	day^{-1}	N
47	K_d(NO_2)	Oxidation rate of NO_2-N to NO_3-N at 20 ^{0}C in reservoir or sluice	day^{-1}	N
48	K_d(orgN)	Hydrolysis rate of organic N to NH_4-N at 20 ^{0}C in reservoir or sluice	day^{-1}	N
49	K_d(orgP)	Hydrolysis rate of organic P to soluble P at 20 ^{0}C in reservoir or sluice	day^{-1}	P
50	K_{scu}(COD)	Resuspension rate of COD at 20 ^{0}C in reservoir or sluice	m/year	COD
51	K_{scu}(NH_4)	Resuspension rate of NH_4-N at 20 ^{0}C in reservoir or sluice	m/year	N
52	K_{scu}(NO_2)	Resuspension rate of NO_2-N at 20 ^{0}C in reservoir or sluice	m/year	N
53	K_{scu}(NO_3)	Resuspension rate of NO_3-N at 20 ^{0}C in reservoir or sluice	m/year	N
54	K_{scu}(orgN)	Resuspension rate of organic N at 20 ^{0}C in reservoir or sluice	m/year	N
55	K_{scu}(orgP)	Resuspension rate of organic P at 20 ^{0}C in reservoir or sluice	m/year	P
56	K_{scu}(solP)	Resuspension rate of soluble P at 20 ^{0}C in reservoir or sluice	m/year	P
57	K_{scu}(DO)	Resuspension rate of DO at 20 ^{0}C in reservoir or sluice	m/year	DO
58	K_{scu}(algae)	Resuspension rate of algae at 20 ^{0}C in reservoir or sluice	m/year	algae
59	K_{scu}(TN)	Resuspension rate of TN at 20 ^{0}C in reservoir or sluice	m/year	N
60	K_{scu}(TP)	Resuspension rate of TP at 20 ^{0}C in reservoir or sluice	m/year	P
61	K_{bur}(COD)	Decay rate of COD at 20 ^{0}C in reservoir or sluice	m/year	COD
62	K_{bur}(NH_4)	Decay rate of NH_4-N at 20 ^{0}C in reservoir or sluice	m/year	N
63	K_{bur}(NO_2)	Decay rate of NO_2-N at 20 ^{0}C in reservoir or sluice	m/year	N
64	K_{bur}(NO_3)	Decay rate of NO_3-N at 20 ^{0}C in reservoir or sluice	m/year	N
65	K_{bur}(orgN)	Decay rate of organic N at 20 ^{0}C in reservoir or sluice	m/year	N
66	K_{bur}(orgP)	Decay rate of organic P at 20 ^{0}C in reservoir or sluice	m/year	P
67	K_{bur}(solP)	Decay rate of soluble P at 20 ^{0}C in reservoir or sluice	m/year	P
68	K_{bur}(DO)	Decay rate of DO at 20 ^{0}C in reservoir or sluice	m/year	DO
69	K_{bur}(algae)	Decay rate of algae at 20 ^{0}C in reservoir or sluice	m/year	algae
70	K_{bur}(TN)	Decay rate of TN at 20 ^{0}C in reservoir or sluice	m/year	N
71	K_{bur} (TP)	Decay rate of TP at 20 ^{0}C in reservoir or sluice	m/year	P
72	*usle_k*	Soil erodibility factor of USLE equation	none	sediment
73	*usle_p*	Erosion control practice factor of USLE equation	none	sediment
74	*MicrIn*	Microbe index	none	C, N
75	K_1	Decomposition rate of labile organic C	day^{-1}	C
76	μ_{CLAY}	Reduction factor of clay content on organic matter decomposition	none	C
77	μ_t	Reduction factor of soil temperature on growth of denitrifier or nitrifier	none	N
78	*S*	Labile fraction of organic C compounds	none	C
79	kr_{cvl}	Decomposition rate of very labile organic C in residue pool	day^{-1}	C
80	kr_{cl}	Decomposition rate of labile organic C in residue pool	day^{-1}	C
81	kr_{cr}	Decomposition rate of stable organic C in residue pool	day^{-1}	C

82	km_{sc}	Decomposition rate of stable organic C in microbial biomass pool	day^{-1}	C
83	km_{cl}	Decomposition rate of labile organic C in microbial biomass pool	day^{-1}	C
84	km_h	Decomposition rate of microbial biomass to humands	day^{-1}	C
85	K_C	Half velocity constant of organic C on denitrifier biomass growth	none	N
86	K_{NxOy}	Half velocity constant of NO_3-N, NO_2-N, NO and N_2O on denitrifier biomass growth	none	N
87	u_{NO3}	Maximum growth rate of NO_3-N denitrifier	day^{-1}	N
88	u_{NO2}	Maximum growth rate of NO_2-N denitrifier	day^{-1}	N
89	u_{NO}	Maximum growth rate of NO denitrifier	day^{-1}	N
90	u_{N2O}	Maximum growth rate of N_2O denitrifier	day^{-1}	N
91	M_C	Maintenance coefficient of C	hr^{-1}	C
92	Y_C	Maximum growth yield of soluble C	kg/ha/hr	C
93	M_{NO3}	Maintenance coefficient of NO_3-N	hr^{-1}	N
94	Y_{NO3}	Maximum growth yield of NO_3-N	kg/ha/hr	N
95	$CDR_{D:N}$	C:N ratio in bacteria	none	N
96	M_{NO2}	Maintenance coefficient of NO_2-N	hr^{-1}	N
97	Y_{NO2}	Maximum growth yield of NO_2-N	kg/ha/hr	N
98	M_{NO}	Maintenance coefficient of NO	hr^{-1}	N
99	Y_{NO}	Maximum growth yield of NO	kg/ha/hr	N
100	M_{N2O}	Maintenance coefficient of N_2O	hr^{-1}	N
101	Y_{N2O}	Maximum growth yield of N_2O	kg/ha/hr	N
102	$\mu_{SW,n}$	Soil water content adjusted factor for denitrification	none	C, N
103	β_{min}	Mineralization rate of humus active organic P	day^{-1}	P
104	β_{rsd}	Mineralization rate of residue fresh organic P	day^{-1}	P
Watershed parameters				
105	C_{ur}(COD)	Export coefficient of COD load in urban area	kg/ha/year	COD
106	C_{ur}(NH_4)	Export coefficient of NH_4-N load in urban area	kg/ha/year	N
107	C_{ur}(TN)	Export coefficient of TN load in urban area	kg/ha/year	N
108	C_{ur}(TP)	Export coefficient of TP load in urban area	kg/ha/year	P
109	C_{ur}(COD)	Export coefficient of COD load in unused area	kg/ha/year	COD
110	C_{ur}(NH_4)	Export coefficient of NH_4-N load in unused area	kg/ha/year	N
111	C_{ur}(TN)	Export coefficient of TN load in unused area	kg/ha/year	N
112	C_{ur}(TP)	Export coefficient of TP load in unused area	kg/ha/year	P
113	R_{ur}	Loss rate of non-point source load from soil layer	none	pollutant load
114	C_{liv}(COD)	Export coefficient of COD load from living in rural area	kg/year	COD
115	C_{liv}(NH_4)	Export coefficient of NH_4-N load from living in rural area	kg/year	N
116	C_{liv}(TN)	Export coefficient of TN load from living in rural area	kg/year	N
117	C_{liv}(TP)	Export coefficient of TP load from living in rural area	kg/year	P
118	C_{lst}(COD)	Export coefficient of COD load from livestock in rural area	kg/year	COD
119	C_{lst}(NH_4)	Export coefficient of NH_4-N load from livestock in rural area	kg/year	N
120	C_{lst}(TN)	Export coefficient of TN load from livestock in rural area	kg/year	N
121	C_{lst}(TP)	Export coefficient of TP load from livestock in rural area	kg/year	P
122	R_{liv}	Loss rate of non-point source load from living	none	pollutant load

123	R_{lst}	Loss rate of non-point source load from livestock	none	pollutant load
124	C_{pcp}(COD)	COD concentration in precipitation	mg/L	COD
125	C_{pcp}(NH_4)	NH_4-N concentration in precipitation	mg/L	N
126	C_{pcp}(TN)	TN concentration in precipitation	mg/L	N
127	C_{pcp}(TP)	TP concentration in precipitation	mg/L	P
128	SF_{tmp}	Snowfall temperature	^{0}C	flow
129	SM_{tmp}	Snow melt base temperature	^{0}C	flow
130	SMF_{mx}	Melt factor for snow on June 21	mm/day	flow
131	SMF_{mn}	Melt factor for snow on December 21	mm/day	flow
132	*TIMP*	Snow pack temperature lag factor	none	flow
133	*Coefrad*	Factor of maximum possible radiation to net radiation	none	flow
134	SC_{max}	Minimum snow water content that corresponds to 100% snow cover	mm	flow
135	SC_{50}	Fraction of snow volume represented by SCMX that corresponds to 50% snow cover	none	flow
136	SC_1	Coefficients that define shape of snow curve 95% coverage at 100% snow cover	none	flow
137	SC_2	Coefficients that define shape of snow curve 50% coverage at 100% snow cover	none	flow
138	*Surlag*	Surface runoff lag time	day	flow
139	*n_ch*	Roughness of Channel	none	flow
140	*msk_x*	Weighting factor in Muskingum equation	none	flow
141	*msk_k*	Storage time constant of channel in Muskingum equation	day	flow
142	AI_1	Fraction of algal biomass that is N	none	N
143	AI_2	Fraction of algal biomass that is P	none	P
144	AI_3	Adjusted rate of oxygen production per unit of algal photolysis	none	DO
145	AI_4	Adjusted rate of oxygen uptake per unit of algal respiration	none	DO
146	AI_5	Adjusted rate of oxygen uptake per unit of NH_4-N oxidation	none	N
147	AI_6	Adjusted rate of oxygen uptake per unit of NO_2-N oxidation	none	N
148	AI_7	Adjusted rate of NH_4-N oxidation to NO_2-N	none	N
149	g_{max}	Maximum specific algal growth rate at 20^{0}C	day^{-1}	algae
150	*RHOQ*	Algal respiration rate at 20^{0}C	day^{-1}	algae
151	*TFACT*	Fraction of solar radiation computed in temperature heat balance	none	algae
152	*K_l*	Half-saturation coefficient for light	kJ/m^2	algae
153	*K_N*	Michaelis-Menton half-saturation constant for N	mg/L	algae
154	*K_P*	Michaelis-Menton half-saturation constant for P	mg/L	algae
155	*Lec*	Non-algal portion of light extinction coefficient	m^{-1}	algae
156	Lec_1	Linear algal self-shading coefficient	$m^{-1\cdot}$ (μg/L)$^{-1}$	algae
157	Lec_2	Nonlinear algal self-shading coefficient	$m^{-1}\cdot$(μg /L)$^{-2/3}$)	algae
158	*P_N*	Algal preference factor for ammonia	none	N
159	*PRF*	Peak rate adjustment factor for sediment routing in channel	none	sediment
160	SP_{con}	Linear parameter for calculating maximum transport capacity of sediment in channel	none	sediment

161	*SPexp*	Exponent parameter for calculating maximum transport capacity of sediment in channel	none	sediment
162	*f_Ph*	Flood PH value	none	C, N
163	rcn_{rvl}	Ratio of C/N of very labile litter	none	C, N
164	rcn_{rl}	Ratio of C/N of labile litter	none	C, N
165	rcn_{rr}	Ratio of C/N of resistant litter	none	C, N
166	rcn_{b}	Ratio of C/N of labile biomass	none	C, N
167	rcn_{h}	Ratio of C/N of labile humus	none	C, N
168	rcn_{m}	Ratio of C/N of humads	none	C, N
169	*pavi*	P availability index	none	C, N
170	*TtoC*	Relationship between TOC and COD	none	COD
171-182	$rpnt_{01\sim12}$	Ratio of point pollutant source from Jan. to Dec.	none	pollutant load

Table S2. The detailed information of data sets for the case study

Category	Data	Spatial scale	Temporal scale	Source
GIS	DEM	Grid: 90m*90 m	none	Institute of Geographic Science and Natural Resources Research, Chinese Academy of Sciences
	Land use	1:1,000,000	none	
	Soil	1:4,000,000	none	
Weather	Precipitation	65 stations	daily (from 2003 to 2008)	Hydrological Yearbooks of Henan Province,China
	Maximum and minimum temperature	6 stations	daily (from 2003 to 2008)	National Meteorological Infomation Center of China
Hydrology	Total runoff, high and low flows	6 stations	daily (from 2003 to 2008)	Hydrological Yearbooks of Henan Province,China
Water quality	Wastewater discharge outlets and the discharge load (wastewater, NH_4-N, etc.)	over 200 outlets	annual (from 2003 to 2008)	Water Resources Protection Bureau of Huai River Basin, China
	Water quality variable concentrations (NH_4-N)	6 stations	daily (from 2003 to 2008)	Water Resources Protection Bureau of Huai River Basin, China
	Nonpoint source load (NH_4-N)	9 administrative regions	average annual (from 2003 to 2005)	Huai River Commission, China
Ecology	Corn yield	9 administrative regions	average annual (from 2003 to 2005)	Henan Statistical Yearbook, China
Economy	Populations in rural area, breeding stock of large animals and livestock, water withdrawal	9 administrative regions	annual (from 2003 to 2008)	Henan Statistical Yearbook, China
Water projects	Water storage capacities of dead, usable, flood control and maximum flood levels and the corresponding water surface areas; the relationship among water level, storage volume and outflow	5 reservoirs and 12 sluices	none	Water Resources Protection Bureau of Huai River Basin, China
Agricultural management	Fertilization and irrigation types, timing and amount, the time of seeding and harvest, crop types	9 administrative regions	average annual (from 2003 to 2008)	Henan Statistical Yearbooks, China,Wang et al., (2008) and Zhai et al. (2014)

Table S3. The agricultural management scheme in the Shaying River Catchment

Crop	Management	Time		Ratio distribution of annual TN fertilizer	Ratio distribution of annual TP fertilizer	Fertilizer intensity (kg/ha)	
		Start (month-day)	Duration (day)			TN	TP
Early rice	Base fertilization	4-1	1	0.60	0.86	40.60-86.17	25.46-59.47
	Plant	4-15	1	-	-		
	Additional Fertilization	5-1	1	0.40	0.14	27.06-57.45	4.14-9.68
	Harvest & Kill	7-31	1	-	-		
Late rice	Base fertilization	8-1	1	0.50	0.86	33.83-71.81	25.46-59.47
	Plant	8-15	1	-	-		
	Additional Fertilization	9-1	1	0.50	0.14	33.83-71.81	4.14-9.68
	Harvest & Kill	10-31	1	-	-		
Winter wheat	Base fertilization	10-1	1	0.64	0.02	43.30-271.04	0.59-4.10
	Plant	10-15	1	-	-		
	Additional Fertilization	1-1	1	0.36	0.98	24.36-152.46	29.00-201.11
	Harvest & Kill	6-1	1	-	-		
Cron	Base fertilization	6-1	1	0.41	0.88	27.74-173.63	26.05-180.59
	Plant	6-15	1	-	-		
	Additional Fertilization	7-15	1	0.59	0.12	39.92-249.86	3.55-24.62
	Harvest & Kill	9-30	1	-	-		